MitoEAGLE preprint 2017-10-13(09)

The protonmotive force and respiratory control:

Building blocks of mitochondrial physiology

Part 1.

http://www.mitoeagle.org/index.php/MitoEAGLE_preprint_2017-09-21

Preprint version 09 (2017-10-13)

MitoEAGLE Network

Corresponding author: Gnaiger E

Contributing co-authors

Ahn B, Alves MG, Amati F, Åsander Frostner E, Bailey DM, Battino M, Beard DA, Ben-Shachar D, Bishop D, Breton S, Brown GC, Brown RA, Buettner GR, Carvalho E, Cervinkova Z, Chicco AJ, Coen PM, Collins JL, Crisóstomo L, Davis MS, Dias T, Distefano G, Doerrier C, Ehinger J, Elmer E, Fell DA, Ferko M, Ferreira JCB, Filipovska A, Fisher J, Garcia-Roves PM, Garcia-Souza LF, Genova ML, Gonzalo H, Goodpaster BH, Gorr TA, Han J, Harrison DK, Hellgren KT, Hernansanz P, Holland O, Hoppel CL, Iglesias-Gonzalez J, Irving BA, Iyer S, Jansen-Dürr P, Jespersen NR, Jha RK, Kaambre T, Kane DA, Kappler L, Keijer J, Komlodi T, Kopitar-Jerala N, Krako Jakovljevic N, Kuang J, Labieniec-Watala M, Lai N, Laner V, Lee HK, Lemieux H, Lerfall J, Lucchinetti E, MacMillan-Crow LA, Makrecka-Kuka M, Meszaros AT, Moisoi N, Molina AJA, Montaigne D, Moore AL, Murray AJ, Newsom S, Nozickova K, O'Gorman D, Oliveira PF, Oliveira PJ, Orynbayeva Z, Pak YK, Palmeira CM, Patel HH, Pesta D, Petit PX, Pichaud N, Pirkmajer S, Porter RK, Pranger F, Prochownik EV, Radenkovic F, Reboredo P, Renner-Sattler K, Robinson MM, Rohlena J, Røsland GV, Rossiter HB, Salvadego D, Scatena R, Schartner M, Scheibye-Knudsen M, Schilling JM, Schlattner U, Schoenfeld P, Scott GR, Singer D, Sobotka O, Spinazzi M, Stier A, Stocker R, Sumbalova Z, Suravajhala P, Tanaka M, Tandler B, Tepp K, Tomar D,

Towheed A, Trivigno C, Tronstad KJ, Trougakos IP, Tyrrell DJ, Velika B, Vendelin M, Vercesi AE, Victor VM, Ward ML, Watala C, Wei YH, Wieckowski MR, Wohlwend M, Wolff J, Wuest RCI, Zaugg K, Zaugg M, Zorzano A

Supporting co-authors:

Arandarčikaitė O, Bakker BM, Bernardi P, Boetker HE, Borsheim E, Borutaitė V, Bouitbir J, Calabria E, Calbet JA, Chaurasia B, Clementi E, Coker RH, Collin A, Das AM, De Palma C, Dubouchaud H, Duchen MR, Durham WJ, Dyrstad SE, Engin AB, Fornaro M, Gan Z, Garlid KD, Garten A, Gourlay CW, Granata C, Haas CB, Haavik J, Haendeler J, Hand SC, Hepple RT, Hickey AJ, Hoel F, Kainulainen H, Keppner G, Khamoui AV, Klingenspor M, Koopman WJH, Kowaltowski AJ, Krajcova A, Lenaz G, Malik A, Markova M, Mazat JP, Menze MA, Methner A, Muntané J, Muntean DM, Neuzil J, Oliveira MT, Pallotta ML, Parajuli N, Pettersen IKN, Pulinilkunnil T, Ropelle ER, Salin K, Sandi C, Sazanov LA, Siewiera K, Silber AM, Skolik R, Smenes BT, Soares FAA, Sokolova I, Sonkar VK, Stankova P, Swerdlow RH, Szabo I, Trifunovic A, Thyfault JP, Tretter L, Vieyra A, Votion DM, Williams C

Updates:

http://www.mitoeagle.org/index.php/MitoEAGLE_preprint_2017-09-21

Correspondence: Gnaiger E
Department of Visceral, Transplant and Thoracic Surgery, D. Swarovski Research Laboratory, Medical University of Innsbruck, Innrain 66/4, A-6020 Innsbruck, Austria
Email: erich.gnaiger@i-med.ac.at
Tel: +43 512 566796, Fax: +43 512 566796 20

This manuscript on 'The protonmotive force and respiratory control' is a position statement in the frame of COST Action CA15203 MitoEAGLE. The list of co-authors evolved from MitoEAGLE Working Group Meetings and a ***bottom-up*** *spirit of COST in phase 1: This is an open invitation to scientists and students to join as co-authors, to provide a balanced view on mitochondrial respiratory control, a fundamental introductory presentation of the concept of the protonmotive force, and a consensus statement on reporting data of mitochondrial respiration in terms of metabolic flows and fluxes. We plan a series of follow-up reports by the expanding MitoEAGLE Network, to increase the scope of recommendations on harmonization and facilitate global communication and collaboration.*

*Phase 2****:*** *MitoEAGLE preprint (Versions 01 – 09): We continue to invite comments and suggestions on the, particularly if you are an* ***early career investigator adding an open future-oriented perspective****, or an* ***established scientist providing a balanced historical basis****. Your critical input into the quality of the manuscript will be most welcome, improving our aims to be educational, general, consensus-oriented, and practically helpful for students working in mitochondrial respiratory physiology.*

Phase 3 (2017-11-11): Manuscript submission to a preprint server, such as BioRxiv. We want to invite further opinion leaders: *To join as a co-author, please feel free to focus on a particular section in terms of direct input and references, contributing to the scope of the manuscript from the perspective of your expertise. Your comments will be largely posted on the discussion page of the MitoEAGLE preprint website.*

If you prefer to submit comments in the format of a referee's evaluation rather than a contribution as a co-author, I will be glad to distribute your views to the updated list of co-authors for a balanced response. We would ask for your consent on this open bottom-up policy.

*Phase 4: We organize a MitoEAGLE session linked to our series of reports at the MiP*conference *Nov 2017 in Hradec Kralove in close association with the MiPsociety (where you hopefully will attend) and at EBEC 2018 in Budapest.*

» http://www.mitoeagle.org/index.php/MiP2017_Hradec_Kralove_CZ

I thank you in advance for your feedback.
With best wishes,

Erich Gnaiger
Chair Mitochondrial Physiology Society - http://www.mitophysiology.org
Chair COST Action MitoEAGLE - http://www.mitoeagle.org
Medical University of Innsbruck, Austria

Contents

Abstract

Clarity of concept and consistency of nomenclature are key trademarks of a research field. These trademarks facilitate effective transdisciplinary communication, education, and ultimately further discovery. As the knowledge base and importance of mitochondrial physiology to human health expand, the necessity for harmonizing nomenclature concerning mitochondrial respiratory states and rates has become increasingly apparent. Peter Mitchell's concept of the protonmotive force establishes the links between electrical and chemical components of energy transformation and coupling in oxidative phosphorylation. This unifying concept provides the framework for developing a consistent nomenclature for mitochondrial physiology and bioenergetics. Herein, we follow IUPAC guidelines on general terms of physical chemistry, extended by the concepts of open systems and irreversible thermodynamics. We align the nomenclature of classical bioenergetics on respiratory states with a concept-driven constructive terminology to address the meaning of each respiratory state. Furthermore, we suggest uniform standards for the evaluation of respiratory states that will ultimately support the development of databases of mitochondrial respiratory function in species, tissues and cells studied under diverse physiological and experimental conditions. In this position statement, in the frame of COST Action CA15203 MitoEAGLE, we endeavour to provide a balanced view on mitochondrial respiratory control, a fundamental introductory presentation of the concept of the protonmotive force, and a critical discussion on reporting data of mitochondrial respiration in terms of metabolic flows and fluxes.

Keywords: Mitochondrial respiratory control, coupling control, mitochondrial preparations, protonmotive force, chemiosmotic theory, oxidative phosphorylation, OXPHOS, efficiency, electron transfer, ET; proton leak, LEAK, residual oxygen consumption, ROX, State 2, State 3, State 4, normalization, flow, flux

Box 1:

In brief: mitochondria and Bioblasts

* Does the public expect biologists to understand Darwin's theory of evolution?
* Do students expect that researchers of bioenergetics can explain Mitchell's theory of chemiosmotic energy transformation?

Mitochondria were described for the first time in 1857 by Rudolph Albert von Kölliker as granular structures or 'sarkosomes'. In 1886 Richard Altman called them 'bioblasts' (published 1894). The word 'mitochondrium' (Greek mitos: thread; chondros: granule) was introduced by Carl Benda (1898). Mitochondria are the oxygen consuming electrochemical generators which evolved from endosymbiotic bacteria (Margulis 1970; Lane 2005). The bioblasts of Richard Altmann (1894) included, not only the mitochondria as presently defined, but also symbiotic and free-living bacteria.

We now recognize mitochondria as dynamic organelles with a double membrane that are contained within eukaryotic cells. The inner mitochondrial membrane shows dynamic tubular and disk-shaped cristae that separate the mitochondrial matrix, *i.e.* the internal mitochondrial compartment, and the intermembrane space; the latter being enclosed by the outer mitochondrial membrane. Mitochondria are the structural and functional elemental units of cell respiration, where cell respiration is defined as the consumption of oxygen coupled to electrochemical proton translocation across the inner mitochondrial membrane. In the process of oxidative phosphorylation (OXPHOS), the reduction of O_2 is electrochemically coupled to the transformation of energy in the form of adenosine triphosphate (ATP; Mitchell 2011). These powerhouses of the cell contain the machinery of the OXPHOS pathway, including transmembrane respiratory complexes (*i.e.* proton pumps with FMN, Fe-S and cytochrome *b*, *c*, aa_3 redox systems); alternative dehydrogenases and oxidases; the coenzyme ubiquinone (coenzyme Q); ATP synthase; the enzymes of the tricarboxylic acid cycle and the fatty acid oxidation enzymes; transporters of ions, metabolites and co-factors; and mitochondrial kinases related to energy transfer pathways. The mitochondrial proteome comprises over 1,200 proteins

198 (MITOCARTA), mostly encoded by nuclear DNA (nDNA), with a variety of functions, many
199 of which are relatively well known (*e.g.* apoptosis-regulating proteins), while others are still
200 under investigation, or need to be identified (*e.g.* alanine transporter).

201 Mitochondria typically maintain several copies of their own genome (hundred to
202 thousands per cell; Cummins 1998), which is almost exclusively maternally inherited (White *et*
203 *al.* 2008) and known as mitochondrial DNA (mtDNA). One exception to strictly maternal
204 inheritance in animals is found in bivalves (Breton *et al.* 2007). mtDNA is 16.5 Kb in length,
205 contains 13 protein-coding genes for subunits of the transmembrane respiratory Complexes CI,
206 CIII, CIV and ATP synthase, and also encodes 22 tRNAs and the mitochondrial 16S and 12S
207 rRNA. The mitochondrial genome is both regulated and supplemented by nuclear-encoded
208 mitochondrial targeted proteins. Evidence has accumulated that additional gene content is
209 encoded in the mitochondrial genome, *e.g.* microRNAs, piRNA, smithRNAs, repeat associated
210 RNA, and even additional proteins (Duarte *et al.* 2014; Lee *et al.* 2015; Cobb *et al.* 2016).

211 The inner mitochondrial membrane contains the non-bilayer phospholipid cardiolipin,
212 which is not present in any other eukaryotic cellular membrane. Cardiolipin promotes the
213 formation of respiratory supercomplexes, which are supramolecular assemblies based upon
214 specific, though dynamic, interactions between individual respiratory complexes (Greggio *et*
215 *al.* 2017; Lenaz *et al.* 2017). Membrane fluidity is an important parameter influencing
216 functional properties of proteins incorporated in the membranes (Waczulikova *et al.* 2007).
217 There is a constant crosstalk between mitochondria and the other cellular components,
218 maintaining cellular mitostasis through regulation at both the transcriptional and post-
219 translational level, and through cell signalling including proteostatic (e.g. the ubiquitin-
220 proteasome and autophagy-lysosome pathways) and genome stability modules thoughout the
221 cell cycle or even cell death, contributing to homeostatic regulation in response to varying
222 energy demands and stress (Quiros *et al.* 2016). In addition to mitochondrial movement along
223 the microtubules, mitochondrial morphology can change in response to the energy requirements

of the cell via processes known as fusion and fission, through which mitochondria can communicate within a network, and in response to intracellular stress factors causing swelling and ultimately permeability transition.

Mitochondrial dysfunction is associated with a wide variety of genetic and degenerative diseases. Robust mitochondrial function is supported by physical exercise and caloric balance, and is central for sustained metabolic health throughout life. Therefore, a better understanding of mitochondrial physiology will improve our understanding of the etiology of disease, the diagnostic repertoire of mitochondrial medicine, with a focus on protective medicine, lifestyle and healthy aging.

Abbreviation: mt, as generally used in mtDNA. Mitochondrion is singular and mitochondria is plural.

'*For the physiologist, mitochondria afforded the first opportunity for an experimental approach to structure-function relationships, in particular those involved in active transport, vectorial metabolism, and metabolic control mechanisms on a subcellular level*' (Ernster and Schatz 1981).

---

1. Introduction

Mitochondria are the powerhouses of the cell with numerous physiological, molecular, and genetic functions (**Box 1**). Every study of mitochondrial function and disease is faced with **E**volution, **A**ge, **G**ender and sex, **L**ifestyle, and **E**nvironment (EAGLE) as essential background conditions intrinsic to the individual patient or subject, cohort, species, tissue and to some extent even cell line. As a large and highly coordinated group of laboratories and researchers, the mission of the global MitoEAGLE Network is to generate the necessary scale, type, and quality of consistent data sets and conditions to address this intrinsic complexity. Harmonization of experimental protocols and implementation of a quality control and data management system is required to interrelate results gathered across a spectrum of studies and to generate a

rigorously monitored database focused on mitochondrial respiratory function. In this way, researchers within the same and across different disciplines will be positioned to compare their findings to an agreed upon set of clearly defined and accepted international standards.

Reliability and comparability of quantitative results depend on the accuracy of measurements under strictly-defined conditions. A conceptually clearly-defined framework is also required to warrant meaningful interpretation and comparability of experimental outcomes carried out by research groups at different institutes. With an emphasis on quality of research, collected data can be useful far beyond the specific question of a specific experiment. Thus enabling meta-analytic studies is the most economic way of providing robust answers to biological questions (Cooper *et al.* 2009). Vague or ambiguous jargon can lead to confusion and may relegate valuable signals to wasteful noise. For this reason, measured values must be expressed in standardized units for each parameter used to define mitochondrial respiratory function. Standardization of nomenclature and technical terms is essential to improve the awareness of the intricate meaning of a divergent scientific vocabulary. The focus on coupling states, the protonmotive force and fluxes through metabolic pathways of aerobic energy transformation in mitochondrial preparations is a first step in the attempt to generate a harmonized and conceptually-oriented nomenclature in bioenergetics and mitochondrial physiology. Coupling states of intact cells and respiratory control by fuel substrates and specific inhibitors of respiratory enzymes will be reviewed in subsequent communications.

2. Respiratory coupling states in mitochondrial preparations

> '*Every professional group develops its own technical jargon for talking about matters of critical concern ... People who know a word can share that idea with other members of their group, and a shared vocabulary is part of the glue that holds people together and allows them to create a shared culture*' (Miller 1991).

Mitochondrial preparations are defined as either isolated mitochondria, or tissue and cellular preparations in which the barrier function of the plasma membrane is disrupted. The plasma membrane separates the cytosol, nucleus, and organelles (the intracellular compartment) from the environment of the cell. The plasma membrane consists of a lipid bilayer, embedded proteins, and attached organic molecules that collectively control the selective permeability of ions, organic molecules, and particles across the cell boundary. The intact plasma membrane, therefore, prevents the passage of many water-soluble mitochondrial substrates, such as succinate or adenosine diphosphate (ADP), that are required for the analysis of respiratory capacity at kinetically-saturating concentrations, thus limiting the scope of investigations into mitochondrial respiratory function in intact cells. The cholesterol content of the plasma membrane is high compared to mitochondrial membranes. Therefore, mild detergents, such as digitonin and saponin, can be applied to selectively permeabilize the plasma membrane by interaction with cholesterol and allow free exchange of cytosolic components with ions and organic molecules of the immediate cell environment, while maintaining the integrity and localization of organelles, cytoskeleton, and the nucleus. Application of optimum concentrations of these mild detergents leads to the complete loss of cell viability, tested by nuclear staining, while mitochondrial function remains unaffected, as shown by an unaltered respiration rate of mitochondria after the addition of such low concertations of digitonin and saponin. In addition to mechanical permeabilization during homogenization of fresh tissue, saponin may be applied to ensure permeabilization of all cells. Crude homogenate and cells permeabilized in the respiration chamber contain all components of the cell at highly diluted concentrations. All mitochondria are retained in chemically-permeabilized mitochondrial preparations and crude tissue homogenates. In the preparation of isolated mitochondria, the cells or tissues are homogenized, and the mitochondria are separated from other cell fractions and purified by differential centrifugation, entailing the loss of a significant fraction of

mitochondria. The term mitochondrial preparation does not include further fractionation of mitochondrial components, as well as submitochondrial particles.

2.1. Three coupling states of mitochondrial preparations and residual oxygen consumption

Respiratory capacities in coupling control states: To extend the classical nomenclature on mitochondrial coupling states (Section 2.4) by a concept-driven terminology that incorporates explicit information on the nature of the respiratory states, the terminology must be general and not restricted to any particular experimental protocol or mitochondrial preparation (Gnaiger 2009). We focus primarily on the conceptual 'why', along with clarification of the experimental 'how'. In the following section, the concept-driven terminology is explained and coupling states are defined. We define respiratory capacities, comparable to channel capacity in information theory (Schneider 2006), as the upper bound of the rate of respiration measured in defined coupling and pathway control states of mitochondrial preparations. To provide a diagnostic reference for respiratory capacities of core energy metabolism, the capacity of *oxidative phosphorylation*, OXPHOS, is measured at kinetically-saturating concentrations of ADP and inorganic phosphate, P_i. The *oxidative* capacity of the electron transfer-pathway, ET-pathway, reveals the limitation of OXPHOS capacity mediated by the *phosphorylation* pathway. The ET and phosphorylation pathways comprise coupled segments of the OXPHOS pathway. ET capacity is measured as noncoupled respiration by application of *external uncouplers*. The contribution of *intrinsically uncoupled* oxygen consumption is most easily studied by not stimulating or arresting phosphorylation, when oxygen consumption compensates mainly for the proton leak; the corresponding states are collectively classified as LEAK states (**Table 1**). Fuel substrates and ET inhibitors are kept constant, *i.e.* maintaining a defined ET-pathway state, while (*1*) adding ADP or P_i, (*2*) inhibiting the phosphorylation pathway, and (*3*) performing uncoupler titrations to induce different coupling states (**Fig. 1**).

Kinetic control: Coupling control states are established in the study of mitochondrial preparations to obtain reference values for various output variables. Physiological conditions *in vivo* may deviate substantially from these experimentally obtained states. Since kinetically-saturating concentrations, *e.g.* of ADP or oxygen, may not apply to physiological intracellular conditions, relevant information is obtained in studies of kinetic responses to conditions intermediate between the LEAK state at zero [ADP] and the OXPHOS state at saturating [ADP], or of respiratory capacities in the range between kinetically-saturating [O_2] and anoxia (Gnaiger 2001).

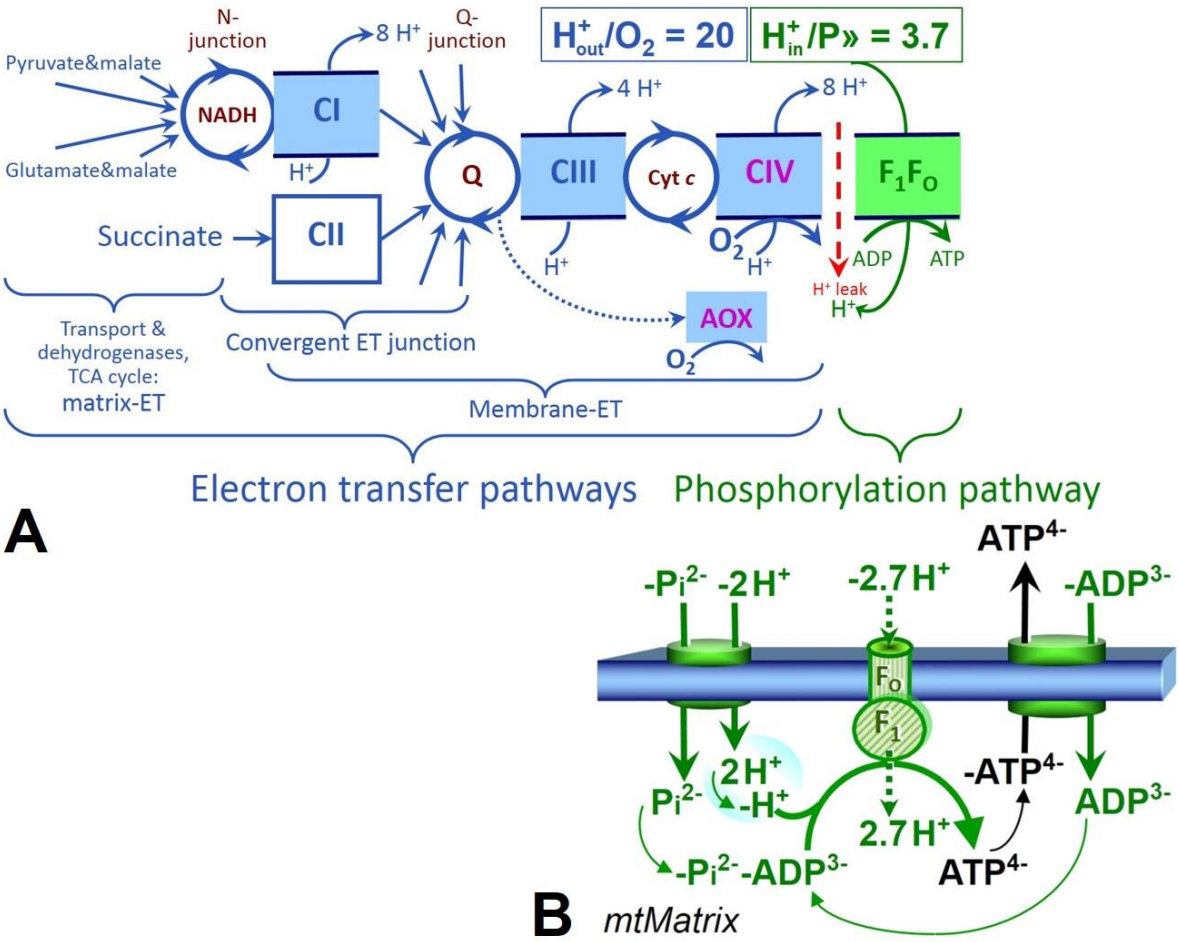

Fig. 1. The oxidative phosphorylation pathway, OXPHOS pathway. (A) Electron transfer, ET, coupled to phosphorylation. Multiple convergent electron transfer pathways are shown from NADH and succinate; additional arrows indicate electron entry through electron transferring flavoprotein, glycerophosphate dehydrogenase, dihydro-orotate dehydrogenase, choline dehydrogenase, and sulfide-ubiquinone oxidoreductase. The branched pathway of oxygen consumption by alternative quinol

oxidase (AOX) is indicated by the dotted arrow. H^+_{out}/O_2 is the ratio of outward proton flux from the matrix space to catabolic O_2 flux in the NADH-linked pathway. $H^+_{in}/P»$ is the ratio of inward proton flux from the inter-membrane space to the flux of phosphorylation of ADP to ATP. Due to proton leak and slip these are not fixed stoichiometries. (**B**) Phosphorylation pathway catalyzed by the F_1F_O ATP synthase, adenine nucleotide translocase, and inorganic phosphate transporter. The $H^+_{in}/P»$ stoichiometry is the sum of the coupling stoichiometry in the ATP synthase reaction (-2.7 H^+ from the intermembrane space, 2.7 H^+ to the matrix) and the proton balance in the translocation of ADP^{2-}, ATP^{3-} and P_i^{2-}. See Eqs. 3 and 4 for further explanation. Modified from (A) Lemieux *et al*. (2017) and (B) Gnaiger (2014).

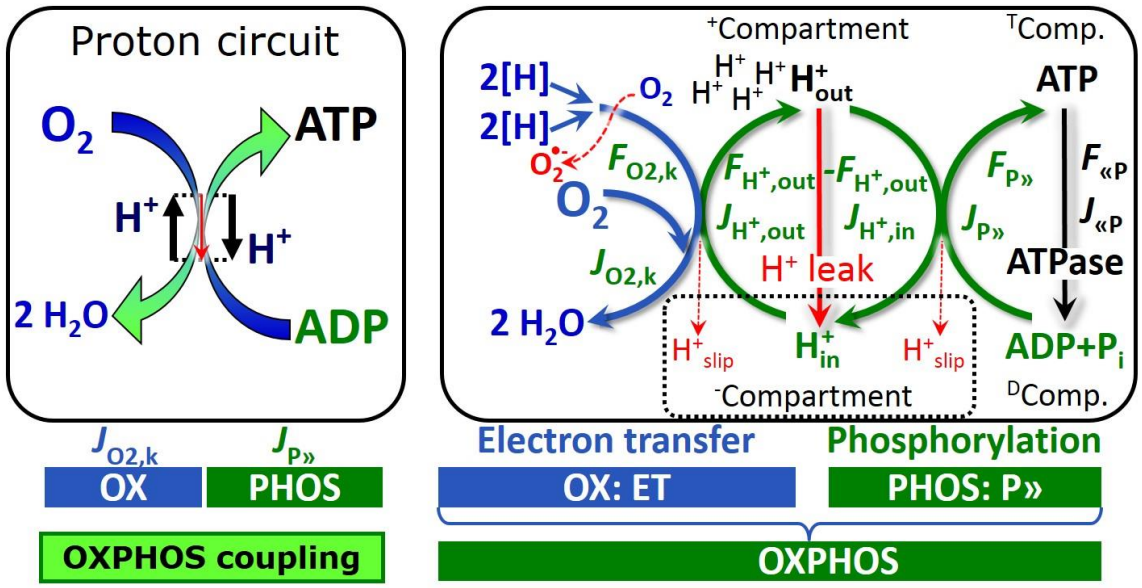

Fig. 2. The proton circuit and coupling in oxidative phosphorylation (OXPHOS). Oxygen flux, $J_{O2,k}$, through the catabolic electron transfer (ET) pathway k is coupled to flux through the phosphorylation pathway of ADP to ATP, $J_{P»}$, by the proton pumps of the ET-pathway, pushing the outward proton flux, $J_{H+,out}$, and generating the output protonmotive force, $F_{H+,out}$. ATP synthase is coupled to inward proton flux, $J_{H+,in}$, to phosphorylate ADP with inorganic phosphate to ATP, driven by the input protonmotive force, $F_{H+,in} = -F_{H+,out}$. 2[H] indicates the reduced hydrogen equivalents of fuel substrates that provide the chemical input force, $F_{O2,k}$ [kJ/mol O_2], of the catabolic reaction k with oxygen (Gibbs energy of reaction per mole O_2 consumed in reaction k), typically in the range of -460 to -480 kJ/mol. The output force is given by the phosphorylation potential difference (ADP phosphorylated to ATP), $F_{P»}$, which varies *in vivo* ranging from about 48 to 62 kJ/mol under physiological conditions. Fluxes, J_B, and forces, F_B, are expressed in either chemical units, [mol·s^{-1}·m^{-3}] and [J·mol^{-1}] respectively, or electrical units,

362 [$C \cdot s^{-1} \cdot m^{-3}$] and [$J \cdot C^{-1}$] respectively, per volume, V [m^3], of the system. The system defined by the
363 boundaries shown as a full black line is not a black box, but is analysed as a compartmental system.
364 The negative compartment (N-compartment, enclosed by the dotted line) is the matrix space, separated
365 from the positive compartment ($^+$Compartment) by the inner mitochondrial membrane. ADP+P_i and ATP
366 are the substrate- and product-compartments (scalar ADP and ATP compartments, ^{D}Comp. and
367 ^{T}Comp.), respectively. Chemical potentials of all substrates and products involved in the scalar reactions
368 are measured in the $^+$Compartment for calculation of the scalar forces $F_{O2,k}$ and $F_{P\text{»}} = -F_{\text{«}P}$ (**Box 2**).
369 Modified from Gnaiger (2014).
370
371 **Phosphorylation, P»:** *Phosphorylation* in the context of OXPHOS is defined as
372 phosphorylation of ADP to ATP. On the other hand, the term phosphorylation is used generally
373 in many different contexts, *e.g.* protein phosphorylation. This justifies consideration of a
374 symbol more discriminating and specific than P as used in the P/O ratio (phosphate to atomic
375 oxygen ratio; O = 0.5 O_2), where P indicates phosphorylation of ADP to ATP or GDP to GTP.
376 We propose the symbol P» for the endergonic direction of phosphorylation ADP→ATP, and
377 likewise the symbol «P for the corresponding exergonic hydrolysis ATP→ADP (**Fig. 2; Box**
378 **3**). ATP synthase is the proton pump of the phosphorylation pathway (**Fig. 1B**). P» may also
379 involve substrate-level phosphorylation as part of the tricarboxylic acid cycle (succinyl-CoA
380 ligase) and phosphorylation of ADP catalyzed by phosphoenolpyruvate carboxykinase,
381 adenylate kinase, creatine kinase, hexokinase and nucleoside diphosphate kinase (NDPK).
382 Kinase cycles are involved in intracellular energy transfer and signal transduction for regulation
383 of energy flux. In isolated mammalian mitochondria ATP production catalyzed by adenylate
384 kinase, 2ADP ↔ ATP + AMP, proceeds without fuel substrates in the presence of ADP
385 (Komlódi and Tretter 2017). $J_{P\text{»}}/J_{O2,k}$ (P»/O_2) is two times the 'P/O' ratio of classical
386 bioenergetics. The effective P»/O_2 ratio is diminished by: (*1*) the proton leak across the inner
387 mitochondrial membrane from low pH in the $^+$Compartment to high pH in the negative
388 compartment ($^-$Compartment); (*2*) cycling of other cations; (*3*) proton slip in the proton pumps

when a proton effectively is not pumped; and (*4*) electron leak in the univalent reduction of oxygen (O_2; dioxygen) to superoxide anion radical ($O_2^{\bullet-}$).

Table 1. Coupling states and residual oxygen consumption in mitochondrial preparations in relation to respiration and phosphorylation rate, $J_{O2,k}$ and $J_{P»}$, and protonmotive force, $F_{H+,out}$. Coupling states are established at kinetically-saturating concentrations of fuel substrates and O_2.

State	$J_{O2,k}$	$J_{P»}$	$F_{H+,out}$	Inducing factors	Limiting factors
LEAK	*L*; low proton leak-dependent respiration	0	max.	Proton leak, slip, and cation cycling	$J_{P»}$ = 0: (*1*) without ADP, L_N; (*2*) max. ATP/ADP ratio, L_T; or (*3*) inhibition of the phosphorylation pathway, L_{Omy}
OXPHOS	*P*; high ADP-stimulated respiration	max.	high	Kinetically-saturating [ADP] and [P_i]	$J_{P»}$ by phosphorylation pathway; or $J_{O2,k}$ by ET-pathway capacity
ET	*E*; max. noncoupled respiration	0	low	Optimal external uncoupler concentration for max. oxygen flux	$J_{O2,k}$ by ET-pathway capacity
ROX	*Rox*; min. residual O_2 consumption	0	0	$J_{O2,Rox}$ in non-ET-pathway oxidation reactions	Full inhibition of ET-pathway or absence of fuel substrates

LEAK state (**Fig. 3**): The LEAK state is defined as a state of mitochondrial respiration when O_2 flux mainly compensates for the proton leak in the absence of ATP synthesis, at kinetically-saturating concentrations of O_2 and respiratory substrates. LEAK respiration is measured to obtain an indirect estimate of *intrinsic uncoupling* without addition of any experimental uncoupler: (*1*) in the absence of adenylates; (*2*) after depletion of ADP at maximum ATP/ADP ratio; or (*3*) after inhibition of the phosphorylation pathway by inhibitors of ATP synthase, such as oligomycin, or adenine nucleotide translocase, such as carboxyatractyloside.

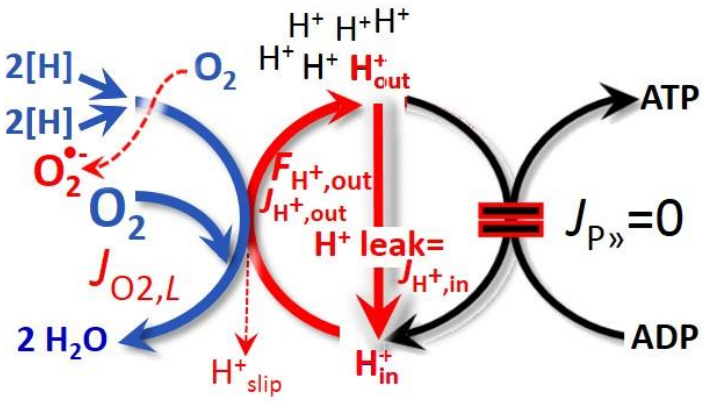

Fig. 3. LEAK state: Phosphorylation is arrested, $J_{P»} = 0$, and oxygen flux, $J_{O2,L}$, is controlled mainly by the proton leak, which equals $J_{H+,in}$, at maximum protonmotive force, $F_{H+,out}$ (See also Fig. 2).

Table 2. Distinction of terms related to coupling.

Term	Respiration	P»/O_2	Note
Fully coupled	*P* – *L*	max.	OXPHOS capacity corrected for LEAK respiration (**Fig. 6**)
Well coupled	*P*	high	Phosphorylating respiration with a variable intrinsic LEAK component (**Fig. 4**)
Loosely coupled	up to *E*	low	Inducibly uncoupled by UCP1 or Ca^{2+} cycling
Dyscoupled	*P*	low	Pathologically, toxicologically, environmentally increased uncoupling, mitochondrial dysfunction
Uncoupled and decoupled	*L*	0	Non-phosphorylating intrinsic LEAK respiration without added protonophore (**Fig. 3**)
Noncoupled	*E*	0	Non-phosphorylating respiration stimulated to maximum flux at optimum exogenous uncoupler concentration (**Fig. 5**)

Proton leak: Proton leak is the *uncoupled* process in which protons are translocated across the inner mitochondrial membrane in the dissipative direction of the downhill protonmotive force without coupling to phosphorylation (**Fig. 3**). The proton leak flux depends on the protonmotive force, is a property of the inner mitochondrial membrane, may be enhanced due to possible contaminations by free fatty acids, and is physiologically controlled. In particular, inducible uncoupling mediated by uncoupling protein 1 (UCP1) is physiologically controlled, *e.g.*, in brown adipose tissue. UCP1 is a proton channel of the inner mitochondrial membrane facilitating the conductance of protons across the inner mitochondrial membrane (Klingenberg 2017). As a consequence of this effective short-circuit, the protonmotive force diminishes, resulting in stimulation of electron transfer to oxygen and heat dissipation without phosphorylation of ADP. Mitochondrial injuries may lead to *dyscoupling* as a pathological or toxicological cause of *uncoupled* respiration, *e.g.*, as a consequence of opening the permeability transition pore. Dyscoupled respiration is distinguished from the experimentally induced *noncoupled* respiration in the ET state. Under physiological conditions, the proton leak is the dominant contributor to the overall leak current (Dufour *et al.* 1996).

Proton slip: Proton slip is the *decoupled* process in which protons are only partially translocated by a proton pump of the ET-pathways and slip back to the original compartment (Dufour *et al.* 1996). Proton slip can also happen in association with the ATP-synthase, in which case the proton slips downhill across the membrane to the matrix without contributing to ATP synthesis. In each case, proton slip is a property of the proton pump and increases with the turnover rate of the pump.

Cation cycling: Proton leak is a leak current of protons. There can be other cation contributors to leak current including calcium and probably magnesium. Calcium current is balanced by mitochondrial Na/Ca exchange, which is balanced by Na/H exchange or K/H exchange. This is another effective uncoupling mechanism different from proton leak and slip.

Small differences of terms, *e.g.*, uncoupled, noncoupled, are easily overlooked and may be erroneously perceived as identical. Even with an attempt at rigorous definition, the common use of such terms may remain vague (**Table 2**).

OXPHOS state (**Fig. 4**): The OXPHOS state is defined as the respiratory state with kinetically-saturating concentrations of O_2, respiratory and phosphorylation substrates, and absence of exogenous uncoupler, which provides an estimate of the maximal respiratory capacity in the OXPHOS state for any given ET-pathway state. Respiratory capacities at kinetically-saturating substrate concentrations provide reference values or upper limits of performance, aiming at the generation of data sets for comparative purposes. Any effects of substrate kinetics are thus separated from reporting actual mitochondrial capacity for oxidation during coupled respiration, against which physiological activities can be evaluated.

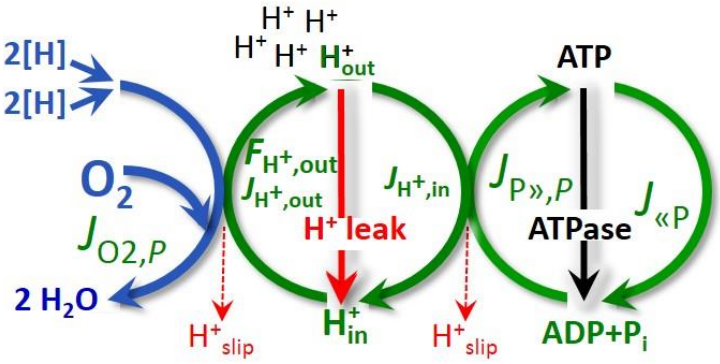

Fig. 4. OXPHOS state: Phosphorylation, $J_{P»}$, is stimulated by kinetically-saturating [ADP] and inorganic phosphate, [P_i], and is supported by a high protonmotive force, $F_{H+,out}$. O_2 flux, $J_{O2,P}$, is highly coupled at a maximum P»/O_2 ratio, $J_{P»,P}/J_{O2,P}$ (See also Fig. 2).

As discussed previously, 0.2 mM ADP does not fully saturate flux in isolated mitochondria (Gnaiger 2001; Puchowicz *et al.* 2004); greater ADP concentration is required, particularly in permeabilized muscle fibres and cardiomyocytes, to overcome limitations by intracellular diffusion and by the reduced conductance of the outer mitochondrial membrane (Jepihhina *et al.* 2011, Illaste *et al.* 2012, Simson *et al.* 2016) either through interaction with tubulin (Rostovtseva *et al.* 2008) or other intracellular structures (Birkedal *et al.* 2014). In permeabilized muscle fibre bundles of high respiratory capacity, the apparent K_m for ADP increases up to 0.5 mM (Saks *et al.* 1998), indicating that >90% saturation is reached only at

466 >5 mM ADP. Similar ADP concentrations are also required for accurate determination of
467 OXPHOS capacity in human clinical cancer samples and permeabilized cells (Klepinin *et al.*
468 2016; Koit *et al.* 2017). Whereas 2.5 to 5 mM ADP is sufficient to obtain the actual OXPHOS
469 capacity in many types of permeabilized cell and tissue preparations, experimental validation
470 is required in each specific case.

471 **Electron transfer state**
472 (**Fig. 5**): The ET state is defined
473 as the *noncoupled* state with
474 kinetically-saturating
475 concentrations of O_2, respiratory
476 substrate and optimum
477 *exogenous* uncoupler
478 concentration for maximum O_2
479 flux, as an estimate of oxidative

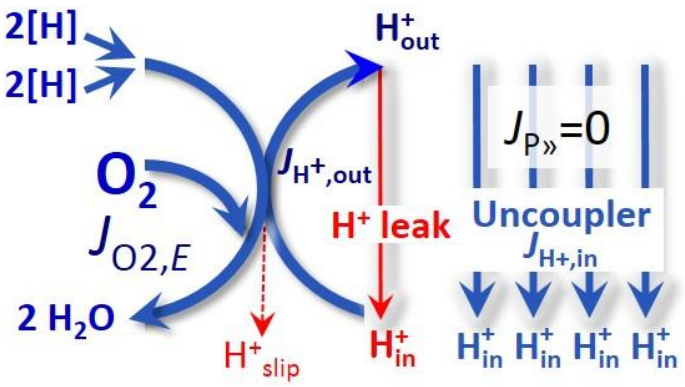

Fig. 5. ET state: Noncoupled respiration, $J_{O2,E}$, is maximum at optimum exogenous uncoupler concentration and phosphorylation is zero, $J_{P»} = 0$ (See also Fig. 2).

480 ET capacity. Inhibition of respiration is observed at higher than optimum uncoupler
481 concentrations. As a consequence of the nearly collapsed protonmotive force, the driving force
482 is insufficient for phosphorylation and $J_{P»} = 0$.

483 Besides the three fundamental coupling states of mitochondrial preparations, the
484 following respiratory state also is relevant to assess respiratory function:

485 **ROX:** Residual oxygen consumption (ROX) is defined as O_2 consumption due to
486 oxidative side reactions remaining after inhibition of ET with rotenone, malonic acid and
487 antimycin A. Cyanide and azide not only inhibit CIV but several peroxidases which might be
488 involved in ROX. ROX is not a coupling state but represents a baseline that is used to correct
489 mitochondrial respiration in defined coupling states. ROX is not necessarily equivalent to non-
490 mitochondrial respiration, considering oxygen-consuming reactions in mitochondria not related
491 to ET, such as oxygen consumption in reactions catalyzed by monoamine oxidases (type A and

B), monooxygenases (cytochrome P450 monooxygenases), dioxygenase (sulfur dioxygenase and trimethyllysine dioxygenase), several hydoxylases, and more. Mitochondrial preparations, especially those obtained from liver, are contaminated by peroxisomes. This fact makes the exact determination of mitochondrial oxygen consumption and mitochondria-associated generation of reactive oxygen species complicated (Schönfeld *et al.* 2009). The dependence of ROX-linked oxygen consumption needs to be studied in detail with respect to non-ET enzyme activities, availability of specific substrates, oxygen concentration, and electron leakage leading to the formation of reactive oxygen species.

2.2. Coupling states and respiratory rates

It is important to distinguish metabolic pathways from metabolic states and the corresponding metabolic rates; for example: electron transfer pathways (**Fig. 6**), ET state (**Fig. 5**), and ET capacity, *E*, respectively (**Table 1**). The protonmotive force is *high* in the OXPHOS state when it drives phosphorylation, *maximum* in the LEAK state of coupled mitochondria, driven by LEAK respiration at a minimum back flux of protons to the matrix side, and *very low* in the ET state when uncouplers short-circuit the proton cycle (**Table 1**).

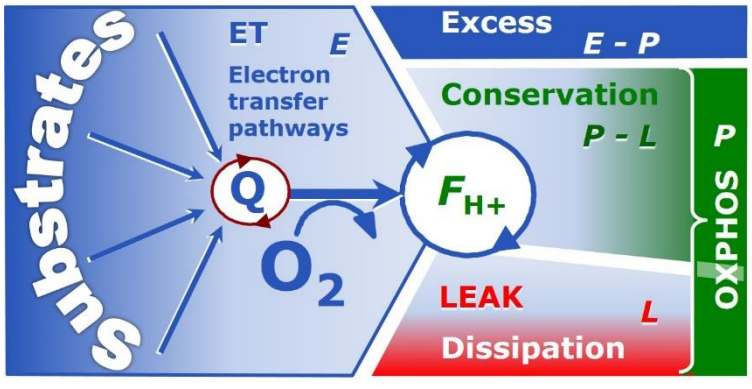

Fig. 6. Four-compartment model of oxidative phosphorylation. Respiratory states (ET, OXPHOS, LEAK) and corresponding rates (*E*, *P*, *L*) are connected by the protonmotive force, $F_{H+,out}$. Electron transfer capacity, *E*, is partitioned into (*1*) dissipative LEAK respiration, *L*, when the capacity to perform work is irreversibly lost, (*2*) net OXPHOS capacity, *P*-*L*, with partial conservation of the capacity to perform work, and (*3*) the excess capacity, *E*-*P*. Modified from Gnaiger (2014).

The three coupling states, ET, LEAK and OXPHOS, are presented in a schematic context with the corresponding respiratory rates, abbreviated as *E*, *L* and *P*, respectively (**Fig. 6**). This clarifies that *E* may exceed or be equal to *P*, but *E* cannot theoretically be lower than *P*. $E < P$ must be discounted as an artefact, which may be caused experimentally by: (*1*) loss of oxidative capacity during the time course of the respirometric assay, since *E* is measured subsequently to *P*; (*2*) using insuffient uncoupler concentrations; (*3*) using high uncoupler concentrations which inhibit ET (Gnaiger 2008); (*4*) high oligomycin concentrations applied for measurement of *L* before titrations of uncoupler, when oligomycin exerts an inhibitory effect on *E*. On the other hand, the excess ET capacity is overestimated if non-saturating [P_i] or [ADP] are used (see State 3 in the next section).

$E > P$ is observed in many types of mitochondria, varying between species, tissues and cell types. It is the excess ET capacity pushing the phosphorylation pathway flux (**Fig. 1B**) to the limit of its *capacity of utilizing* the protonmotive force. Within any type of mitochondria, the magnitude of $E > P$ depends on (*1*) the pathway control state with single or multiple electron input into the Q-junction and involvement of three or fewer coupling sites determining the H^+_{out}/O_2 *coupling stoichiometry* (**Fig. 1A**); and (*2*) the *biochemical coupling efficiency* expressed as *(E-L)/E*, since an increase of *L* causes *P* to increase towards the limit of *E*. The *excess E-P* capacity, *E-P*, therefore, provides a sensitive diagnostic indicator of specific injuries of the phosphorylation pathway, under conditions when *E* remains constant but *P* declines relative to controls (**Fig. 6**). Substrate cocktails supporting simultaneous convergent electron transfer to the Q-junction for reconstitution of tricarboxylic acid cycle (TCA cycle) function establish pathway control states with high ET capacity, and consequently increase the sensitivity of the *E-P* assay.

When subtracting *L* from *P*, the dissipative LEAK component in the OXPHOS state may be overestimated. This can be avoided by measuring LEAK respiration in a state when the protonmotive force is adjusted to its slightly lower value in the OXPHOS state, *e.g.*, by titration

of an ET inhibitor. Any turnover-dependent components of proton leak and slip, however, are underestimated under these conditions (Garlid *et al.* 1993). In general, it is inappropriate to use the term *ATP production* or *ATP turnover* for the difference of oxygen consumption measured in states *P* and *L*. The difference *P-L* is the upper limit of the part of OXPHOS capacity that is freely available for ATP production (corrected for LEAK respiration) and is fully coupled to phosphorylation with a maximum mechanistic stoichiometry (**Fig. 6**).

2.3. Classical terminology for isolated mitochondria

> *'When a code is familiar enough, it ceases appearing like a code; one forgets that there is a decoding mechanism. The message is identical with its meaning'* (Hofstadter 1979).

Chance and Williams (1955; 1956) introduced five classical states of mitochondrial respiration and cytochrome redox states. **Table 3** shows a protocol with isolated mitochondria in a closed respirometric chamber, defining a sequence of respiratory states.

Table 3. Metabolic states of mitochondria (Chance and Williams, 1956; Table V).

State	$[O_2]$	ADP level	Substrate level	Respiration rate	Rate-limiting substance
1	>0	low	low	slow	ADP
2	>0	high	~0	slow	substrate
3	>0	high	high	fast	respiratory chain
4	>0	low	high	slow	ADP
5	0	high	high	0	oxygen

State 1 is obtained after addition of isolated mitochondria to air-saturated isoosmotic/isotonic respiration medium containing inorganic phosphate, but no fuel substrates and no adenylates, *i.e.*, AMP, ADP, ATP.

State 2 is induced by addition of a high concentration of ADP (typically 100 to 300 µM), which stimulates respiration transiently on the basis of endogenous fuel substrates and

phosphorylates only a small portion of the added ADP. State 2 is then obtained at a low respiratory activity limited by zero endogenous fuel substrate availability (**Table 3**). If addition of specific inhibitors of respiratory complexes, such as rotenone, does not cause a further decline of oxygen consumption, State 2 is equivalent to residual oxygen consumption (See below). If inhibition is observed, undefined endogenous fuel substrates are a confounding factor of pathway control by externally added substrates and inhibitors. In contrast to the original protocol, an alternative sequence of titration steps is frequently applied, in which the alternative State 2 has an entirely different meaning, when this second state is induced by addition of fuel substrate without ADP (LEAK state; in contrast to State 2 defined in **Table 2** as a ROX state), followed by addition of ADP.

State 3 is the state stimulated by addition of fuel substrates while the ADP concentration is still high (**Table 3**) and supports coupled energy transformation through oxidative phosphorylation. 'High ADP' is a concentration of ADP specifically selected to allow the measurement of State 3 to State 4 transitions of isolated mitochondria in a closed respirometric chamber. Repeated ADP titration re-establishes State 3 at ‘high ADP’. Starting at oxygen concentrations near air-saturation (ca. 200 µM O_2 at sea level and 37 °C), the total ADP concentration added must be low enough (typically 100 to 300 µM) to allow phosphorylation to ATP at a coupled oxygen consumption that does not lead to oxygen depletion during the transition to State 4. In contrast, kinetically-saturating ADP concentrations usually are an order of magnitude higher than 'high ADP', *e.g.* 2.5 mM in isolated mitochondria. The abbreviation State 3u is frequently used in bioenergetics, to indicate the state of respiration after titration of an uncoupler, without sufficient emphasis on the fundamental difference between OXPHOS capacity (*well-coupled* with an *endogenous* uncoupled component) and ET capacity (*noncoupled*).

State 4 is a LEAK state that is obtained only if the mitochondrial preparation is intact and well-coupled. Depletion of ADP by phosphorylation to ATP leads to a decline in oxygen

595 consumption in the transition from State 3 to State 4. Under these conditions, a maximum
596 protonmotive force and high ATP/ADP ratio are maintained, and the P»/O_2 ratio can be
597 calculated. State 4 respiration, L_T (**Table 1**), reflects intrinsic proton leak and intrinsic ATP
598 hydrolysis activity. Oxygen consumption in State 4 is an overestimation of LEAK respiration
599 if the contaminating ATP hydrolysis activity recycles some ATP to ADP, $J_{«P}$, which stimulates
600 respiration coupled to phosphorylation, $J_{P»} > 0$. This can be tested by inhibition of the
601 phosphorylation pathway using oligomycin, ensuring that $J_{P»} = 0$ (State 4o). Alternatively,
602 sequential ADP titrations re-establish State 3, followed by State 3 to State 4 transitions while
603 sufficient oxygen is available. However, anoxia may be reached before exhaustion of ADP
604 (State 5).

605 **State 5** is the state after exhaustion of oxygen in a closed respirometric chamber.
606 Diffusion of oxygen from the surroundings into the aqueous solution may be a confounding
607 factor preventing complete anoxia (Gnaiger 2001). Chance and Williams (1955) provide an
608 alternative definition of State 5, which gives it the meaning of ROX: 'State 5 may be obtained
609 by antimycin A treatment or by anaerobiosis'.

610 In **Table 3**, only States 3 and 4 (and 'State 2' in the alternative protocol without ADP;
611 not included in the table) are coupling control states, with the restriction that O_2 flux in State 3
612 may be limited kinetically by non-saturating ADP concentrations (**Table 1**).

613

614 **3. The protonmotive force and proton flux**

615 *3.1. Electric and chemical partial forces versus electrical and chemical units*

616 The protonmotive force across the inner mitochondrial membrane (Mitchell and Moyle
617 1967) was introduced most beautifully in the *Grey Book 1966* (see Mitchell 2011),

618 $$\Delta p_{H+} = \Delta\Psi + \Delta\mu_{H+}/F \qquad \text{(Eq. 1)}$$

619 The protonmotive force consists of two partial forces: (*1*) The electrical part, $\Delta\Psi$, is the
620 difference of charge (electric potential difference) and is not specific for H^+. (*2*) The chemical

621 part, $\Delta\mu_{H+}$, is the chemical potential difference in H^+, is proportional to the pH difference, and
622 incorporates the Faraday constant (**Table 4**).

623

624 **Table 4. Protonmotive force and flux matrix.** Rows: Electrical and chemical
625 isomorphic format (*e* and *n*). The Faraday constant, *F*, converts protonmotive force
626 and flux from *isomorphic format e* to *n*. Columns: The protonmotive force is the sum of
627 *partial isomorphic forces* F_{el} and $F_{H+,d}$. In contrast to force (state), the conjugated flux
628 (rate) cannot be partitioned.
629

State		Force		electric	+	chem.	Unit	Notes
	Protonmotive force, *e*	Δp_{H+}	=	$\Delta\Psi$	+	$\Delta\mu_{H+}/F$	$J\cdot C^{-1}$	1*e*
	Chemiosmotic potential, *n*	$\Delta\tilde{\mu}_{H+}$	=	$\Delta\Psi\cdot F$	+	$\Delta\mu_{H+}$	$J\cdot mol^{-1}$	1*n*
State	**Isomorphic force**	$F_{H+,out/i}$		**el_{out}**	**+**	**$H^+_{out,d}$**		
	Electric charge, *e*	$F_{H+,out/e}$	=	$F_{el,out/e}$	+	$F_{H+,out,d/e}$	$J\cdot C^{-1}$	2*e*
	Amount of substance, *n*	$F_{H+,out/n}$	=	$F_{el,out/n}$	+	$F_{H+,out,d/n}$	$J\cdot mol^{-1}$	2*n*
Rate	**Isomorphic flux**	$J_{H+,out/i}$		***e***	**or**	***n***		
	Electric charge, *e*	$J_{H+,out/e}$		$J_{H+,out/e}$			$C\cdot s^{-1}\cdot m^{-3}$	3*e*
	Amount of substance, *n*	$J_{H+,out/n}$				$J_{H+,out/n}$	$mol\cdot s^{-1}\cdot m^{-3}$	3*n*

630

631 1: The Faraday constant, *F*, is the product of elementary charge (e = $1.602177\cdot10^{-19}$·C) and the
632 Avogadro (Loschmidt) constant (N_A = $6.022136\cdot10^{23}\cdot mol^{-1}$), $F = eN_A$ = 96,485.3 C/mol. $\Delta\tilde{\mu}_{H+}$ is the
633 chemiosmotic potential difference. 1*e* and 1*n* are the classical representations of 2*e* and 2*n*.
634 2: The protonmotive force is $F_{H+,out}$, expressed either in isomorphic format *e* or *n*. $F_{el/e}\equiv\Delta\Psi$ is the partial
635 protonmotive force (el) acting generally on charged motive molecules (*i.e.* ions that are displaceable
636 across the inner mitochondrial membrane). In contrast, $F_{H+,d/n}\equiv\Delta\mu_{H+}$ is the partial protonmotive force
637 specific for proton displacement (H^+_d). The sign of the force is negative for exergonic transformations
638 in which exergy is lost or dissipated, and positive for endergonic transformations which conserve
639 exergy from a coupled exergonic process (**Box 3**).
640 3: The sign of the flux depends on the definition of the compartmental direction of the translocation (**Fig.**
641 **2**). Flux x force = $J_{H+,out/e}\cdot F_{H+,out/e} = J_{H+,out/n}\cdot F_{H+,out/n}$ = volume-specific power [$J\cdot s^{-1}\cdot m^{-3} = W\cdot m^{-3}$].

642

643 **Faraday constant**, $F = eN_A$ [C/mol] (**Table 4**), enables the conversion between
644 protonmotive force, $F_{H+,out/e} \equiv \Delta p_{H+}$ [J/C], expressed per *motive charge*, *e* [C], and protonmotive
645 force or electrochemical potential difference, $F_{H+,out/n} \equiv \Delta\tilde{\mu}_{H+} = \Delta p_{H+} \cdot F$ [J/mol], expressed per
646 *motive amount of protons*, *n* [mol]. Proton charge, *e*, and amount of substance, *n*, define the
647 units for the isomorphic formats. Taken together, *F* converts protonmotive force and flux from
648 isomorphic format *e* to *n* (Eq. 2; see also **Table 4**, Note 2),

649 $$F_{H+,out/n} = F_{H+,out/e} \cdot eN_A \qquad \text{(Eq. 2.1)}$$

650 $$J_{H+,out/n} = J_{H+,out/e} / (eN_A) \qquad \text{(Eq. 2.2)}$$

651 In each format, the protonmotive force is expressed as the sum of two partial forces. The
652 concept expressed by the complex symbols in Eq. 1 can be explained and visualized more easily
653 by *partial isomorphic forces* as the components of the protonmotive force:

654 **Electrical part of the protonmotive force:** (*1*) Isomorph *e:* $F_{el/e} \equiv \Delta\Psi$ is the electrical
655 part of the protonmotive force expressed in units joule per coulomb, *i.e.* volt [V = J/C]. $F_{el/e}$ is
656 defined as partial Gibbs energy change per *motive elementary charge*, *e* [C], not specific for
657 proton charge (**Table 4**, Note 2*e*). (*2*) Isomorph *n:* $F_{el/n} \equiv \Delta\Psi \cdot F$ is the electric force expressed
658 in units joule per mole [J/mol], defined as partial Gibbs energy change per *motive amount of*
659 *charge*, *n* [mol], not specific for proton charge (**Table 4**, Note 2*n*).

660 **Chemical part of the protonmotive force:** (*1*) Isomorph *n:* $F_{d,H+/n} \equiv \Delta\mu_{H+}$ is the chemical
661 part (diffusion, displacement of H^+) of the protonmotive force expressed in units joule per mole
662 [J/mol]. $F_{d,H+/n}$ is defined as partial Gibbs energy change per *motive amount of protons*, *n* [mol]
663 (**Table 4**, Note 2*n*). (*2*) Isomorph *e*: $F_{d,H+/e} \equiv \Delta\mu_{H+}/F$ is the chemical force expressed in units
664 joule per coulomb [V], defined as partial Gibbs energy change per *motive amount of protons*
665 *expressed in units of electric charge, e* [C], but specific for proton charge (**Table 4**, Note 2*e*).

666 Protonmotive means that there is a potential for the movement of protons, and force is a
667 measure of the potential for motion. Motion is relative and not absolute (Principle of Galilean
668 Relativity); likewise there is no absolute potential, but (isomorphic) forces are potential

669 differences. An electric partial force expressed in the format of electric charge, $F_{el/e}$, of -0.2 V
670 (**Table 5**, Note 5*e*) is equivalent to force in the format of amount, $F_{el,H+/n}$, of 19 kJ·mol^{-1} H^+_{out}
671 (Note 5*n*). For a ΔpH of 1 unit, the chemical partial force in the format of amount, $F_{d,H+/n}$,
672 changes by 5.9 kJ·mol^{-1} (**Table 5**, Note 6*n*) and chemical force in the format of charge $F_{d,H+/e}$
673 changes by 0.06 V (Note 6*e*). Considering a driving force of -470 kJ·mol^{-1} O_2 for oxidation, the
674 thermodynamic limit of the H^+_{out}/O_2 ratio is reached at a value of 470/19 = 24, compared to a
675 mechanistic stoichiometry of 20 (**Fig. 1**).
676
677 *3.2. Definitions*
678 **Control and regulation:** The terms metabolic *control* and *regulation* are frequently used
679 synonymously, but are distinguished in metabolic control analysis: 'We could understand the
680 regulation as the mechanism that occurs when a system maintains some variable constant over
681 time, in spite of fluctuations in external conditions (homeostasis of the internal state). On the
682 other hand, metabolic control is the power to change the state of the metabolism in response to
683 an external signal' (Fell 1997). Respiratory control may be induced by experimental control
684 signals that *exert* an influence on: (*1*) ATP demand and ADP phosphorylation rate; (*2*) fuel
685 substrate composition, pathway competition; (*3*) available amounts of substrates and oxygen,
686 *e.g.*, starvation and hypoxia; (*3*) the protonmotive force, redox states, flux-force relationships,
687 coupling and efficiency; (*4*) Ca^{2+} and other ions including H^+; (*5*) inhibitors, *e.g.*, nitric oxide
688 or intermediary metabolites, such as oxaloacetate; (*6*) signalling pathways and regulatory
689 proteins, *e.g.* insulin resistance, transcription factor HIF-1 or inhibitory factor 1. *Mechanisms*
690 of respiratory control and regulation include adjustments of (*1*) enzyme activities by allosteric
691 mechanisms and phosphorylation, (*2*) enzyme content, concentrations of cofactors and
692 conserved moieties (such as adenylates, nicotinamide adenine dinucleotide [NAD^+/NADH],
693 coenzyme Q, cytochrome *c*); (*3*) metabolic channeling by supercomplexes; and *(4)*
694 mitochondrial density (enzyme concentrations and membrane area) and morphology (cristae

folding, fission and fusion). (*5*) Mitochondria are targeted directly by hormones, thereby affecting their energy metabolism (Lee *et al.* 2013; Gerö and Szabo 2016; Price and Dai 2016; Moreno *et al.* 2017). Evolutionary or acquired differences in the genetic and epigenetic basis of mitochondrial function (or dysfunction) between subjects and gene therapy; age; gender, biological sex, and hormone concentrations; life style including exercise and nutrition; and environmental issues including thermal, atmospheric, toxicological and pharmacological factors, exert an influence on all control mechanisms listed above (for reviews, see Brown 1992; Gnaiger 1993a, 2009; 2014; Paradies *et al.* 2014; Morrow *et al*. 2017).

Respiratory control and response: Lack of control by a metabolic pathway, *e.g.* phosphorylation pathway, does mean that there will be no response to a variable activating it, *e.g.* [ADP]. However, the reverse is not true as the absence of a response to [ADP] does not exclude the phosphorylation pathway from having some degree of control. The degree of control of a component of the OXPHOS pathway on an output variable, such as oxygen flux, will in general be different from the degree of control on other outputs, such as phosphorylation flux or proton leak flux (**Box 2**). As such, it is necessary to be specific as to which input and output are under consideration (Fell 1997). Therefore, the term respiratory control is elaborated in more detail in the following section.

Respiratory coupling control: Respiratory control refers to the ability of mitochondria to adjust oxygen consumption in response to external control signals by engaging various mechanisms of control and regulation. Respiratory control is monitored in a mitochondrial preparation under conditions defined as respiratory states. When phosphorylation of ADP to ATP is stimulated or depressed, an increase or decrease is observed in electron flux linked to oxygen consumption in respiratory coupling states of intact mitochondria (‘controlled states’ in the classical terminology of bioenergetics). Alternatively, coupling of electron transfer with phosphorylation is disengaged by disruption of the integrity of the inner mitochondrial membrane or by uncouplers, functioning like a clutch in a mechanical system. The

721 corresponding coupling control state is characterized by high levels of oxygen consumption
722 without control by phosphorylation ('uncontrolled state'). Energetic coupling is defined in **Box**
723 **4**. Loss of coupling lowers the efficiency by intrinsic uncoupling and decoupling, or
724 pathological dyscoupling. Such generalized uncoupling is different from switching to
725 mitochondrial pathways that involve fewer than three proton pumps ('coupling sites':
726 Complexes CI, CIII and CIV), bypassing CI through multiple electron entries into the Q-
727 junction (**Fig. 1**). A bypass of CIII and CIV is provided by alternative oxidases, which reduce
728 oxygen without proton translocation. Reprogramming of mitochondrial pathways may be
729 considered as a switch of gears (changing the stoichiometry) rather than uncoupling (loosening
730 the stoichiometry).

731 **Pathway control states** are obtained in mitochondrial preparations by depletion of
732 endogenous substrates and addition to the mitochondrial respiration medium of fuel substrates
733 (CHNO) and specific inhibitors, activating selected mitochondrial pathways (**Fig. 1**). Coupling
734 control states and pathway control states are complementary, since mitochondrial preparations
735 depend on an exogenous supply of pathway-specific fuel substrates and oxygen (Gnaiger 2014).
736

737 **Box 2: Metabolic fluxes and flows: vectorial and scalar**

738 In mitochondrial electron transfer (**Fig. 1**), vectorial transmembrane proton flux is coupled
739 through the proton pumps CI, CIII and CIV to the catabolic flux of scalar reactions, collectively
740 measured as oxygen flux. In **Fig. 2**, the scalar catabolic reaction, k, of oxygen consumption,
741 $J_{O2,k}$ [mol·s^{-1}·m^{-3}], is expressed as oxygen flux per volume, V [m^3], of the instrumental chamber
742 (the system).

743 Fluxes are *vectors*, if they have *spatial* direction in addition to magnitude. A vector flux
744 (surface-density of flow) is expressed per unit cross-sectional area, A [m^2], perpendicular to the
745 direction of flux. If *flows*, *I*, are defined as extensive quantities of the *system*, as vector or scalar
746 flow, $\boldsymbol{I}$ or I [mol·s^{-1}], respectively, then the corresponding vector and scalar *fluxes*, *J*, are

obtained as $\boldsymbol{J} = \boldsymbol{I} \cdot A^{-1}$ [mol·s^{-1}·m^{-2}] and $J = I \cdot V^{-1}$ [mol·s^{-1}·m^{-3}], respectively, expressing flux as an area-specific vector or volume-specific scalar quantity.

Vectorial transmembrane proton flux, $J_{H+,out}$, is analyzed in a heterogenous compartmental system as a quantity with *directional* but not *spatial* information. Translocation of protons across the inner mitochondrial membrane has a defined direction, either from the negative compartment (matrix space; negative or $^{-}$Compartment) to the positive compartment (inter-membrane space; positive or $^{+}$Compartment) or *vice versa* (**Fig. 2**). The arrows defining the direction of the translocation between the two compartments may point upwards or downwards, right or left, without any implication that these are actual directions in space. The 'upper' compartment of the $^{+}$Compartment is neither above nor below the $^{-}$Compartment in a spatial sense, but can be visualized arbitrarily in a figure as the upper compartment (**Fig. 2**). In general, the *compartmental direction* of vectorial translocation from the $^{-}$Compartment to the $^{+}$Compartment is defined by assigning the initial and final state as *ergodynamic compartments*, $H^{+}_{in} \rightarrow H^{+}_{out}$, respectively, related to work (erg = work) that must be performed to lift the proton from a lower to a higher electrochemical potential or from the lower to the higher ergodynamic compartment (Gnaiger 1993b).

In direct analogy to *vectorial* translocation, the direction of a *scalar* chemical reaction, A → B, is defined by assigning substrates and products, A and B, as ergodynamic compartments. O_2 is defined as a substrate in respiratory O_2 consumption, which together with the fuel substrates comprises the substrate compartment of the catabolic reaction (**Fig. 2**). Volume-specific scalar O_2 flux is coupled (**Box 4**) to vectorial translocation. In order to establish a quantitative relation between the coupled fluxes, both $J_{O2,k}$ and $J_{H+,out}$ must be expressed in identical units ([mol·s^{-1}·m^{-3}] or [C·s^{-1}·m^{-3}]), yielding the H^{+}_{out}/O_2 ratio (**Fig. 1**). The *vectorial* proton flux in compartmental translocation has *compartmental direction*, distinguished from a *vector* flux with *spatial direction*. Likewise, the corresponding protonmotive force is defined

as an electrochemical potential *difference* between two compartments, in contrast to a *gradient* across the membrane or a vector force with defined spatial direction.

The steady-state: Mitochondria represent a thermodynamically open system functioning as a biochemical transformation system in non-equilibrium states. State variables (protonmotive force; redox states) and metabolic fluxes (*rates*) are measured in defined mitochondrial respiratory *states*. Strictly, steady states can be obtained only in open systems, in which changes due to *internal* transformations, *e.g.*, O_2 consumption, are instantaneously compensated for by *external* fluxes *e.g.*, O_2 supply, such that oxygen concentration does not change in the system (Gnaiger 1993b). Mitochondrial respiratory states monitored in closed systems satisfy the criteria of pseudo-steady states for limited periods of time, when changes in the system (concentrations of O_2, fuel substrates, ADP, P_i, H^+) do not exert significant effects on metabolic fluxes (respiration, phosphorylation). Such pseudo-steady states require respiratory media with sufficient buffering capacity and kinetically-saturating concentrations of substrates to be maintained, and thus depend on the kinetics of the processes under investigation. Proton turnover, $J_{\infty H+}$, and ATP turnover, $J_{\infty P}$, proceed in the steady-state at constant $F_{H+,out}$, when $J_{\infty H+} = J_{H+,out} = J_{H+,in}$, and at constant $F_{P»}$, when $J_{\infty P} = J_{P»} = J_{«P}$ (**Fig. 2**).

Box 3: Endergonic and exergonic transformations, exergy and dissipation

A chemical reaction, or any transformation, is exergonic if the Gibbs energy change (exergy) of the reaction is negative at constant temperature and pressure. The sum of Gibbs energy changes of all internal transformations in a system can only be negative, *i.e.* exergy is irreversibly dissipated. Endergonic reactions are characterized by positive Gibbs energies of reaction and cannot proceed spontaneously in the forward direction as defined. For instance, the endergonic reaction P» is coupled to exergonic catabolic reactions, such that the total Gibbs energy change is negative, *i.e.* exergy must be dissipated for the reaction to proceed (**Fig. 2**).

In contrast, energy cannot be lost or produced in any internal process, which is the key message of the first law of thermodynamics. Thus mitochondria are the sites of energy transformation but not energy production. Open and closed systems can gain energy and exergy only by external fluxes, *i.e.* uptake from the environment. Exergy is the potential to perform work. In the framework of flux-force relationships (**Box 4**), the *partial* derivative of Gibbs energy per advancement of a transformation is an isomorphic force, F_{tr} (**Table 5**, Note 2). In other words, force is equal to exergy/motive unit (in integral form, this definition takes care of non-isothermal processes). This formal generalization represents an appreciation of the conceptual beauty of Peter Mitchell's innovation of the protonmotive force against the background of the established paradigm of the electromotive force (emf) defined at the limit of zero current (Cohen *et al.* 2008).

Table 5. Power, exergy, force, flux, and advancement.

Expression	Symbol	Definition	Unit	Notes
Power, volume-specific	$P_{V,tr}$	$P_{V,tr} = J_{tr} \cdot F_{tr} = \partial_{tr}G \cdot \partial t^{-1}$	$W = J \cdot s^{-1} \cdot m^{-3}$	1
Force, isomorphic	F_{tr}	$F_{tr} = \partial_{tr}G \cdot \partial_{tr}\xi^{-1}$	$J \cdot x^{-1}$	2
Flux, isomorphic	J_{tr}	$J_{tr} = d_{tr}\xi \cdot dt^{-1} \cdot V^{-1}$	$x \cdot s^{-1} \cdot m^{-3}$	3
Advancement, *n*	$d_{tr}\xi_{H+/n}$	$d_{tr}\xi_{H+/n} = d_{tr}n_{H+} \cdot \nu_{H+}^{-1}$	mol	4*n*
Advancement, *e*	$d_{tr}\xi_{H+/e}$	$d_{tr}\xi_{H+/e} = d_{tr}e_{H+} \cdot \nu_{H+}^{-1}$	C	4*e*
Electric partial force, *e*	$F_{el/e}$	$F_{el/e} \equiv \Delta\Psi$	V	5*e*
Electric partial force, *n*	$F_{el/n}$	$\Delta\Psi \cdot F = 96.5 \cdot \Delta\Psi$	$kJ \cdot mol^{-1}$	5*n*
Chemical partial force, *e*	$F_{d,H+/e}$	$\Delta\mu_{H+}/F = -\ln(10) \cdot RT/F \cdot \Delta pH$	V	6*e*
at 37 °C		$= -0.06 \cdot \Delta pH$	$J \cdot C^{-1}$	
Chemical partial force, *n*	$F_{d,H+/n}$	$\Delta\mu_{H+} = -\ln(10) \cdot RT \cdot \Delta pH$	$J \cdot mol^{-1}$	6*n*
at 37 °C		$= -5.9 \cdot \Delta pH$	$kJ \cdot mol^{-1}$	

1 to 4: An isomorphic motive entity or transformant, expressed in units x, is defined for any transformation, tr. x = mol or C in proton translocation.

2: $\partial_{tr}G$ [J] is the partial Gibbs energy change in the advancement of transformation tr.

3: For x = C, flow is electric current, I_{el} [A = C·s^{-1}], vector flux is electric current density per area, $\boldsymbol{J}_{el}$, and compartmental flux is electric current density per volume, I_{el} [A·m^{-3}].

4*n*: For a chemical reaction, the advancement of reaction r is $d_r\xi_B = d_rn_B \cdot \nu_B^{-1}$ [mol]. The stoichiometric number is $\nu_B = -1$ or $\nu_B = 1$, depending on B being a product or substrate, respectively, in reaction r involving one mole of B. The conjugated *intensive* molar quantity, $F_{B,r} = \partial_rG/\partial_r\xi_B$ [J·mol^{-1}], is the chemical force of reaction or *reaction-motive* force per stoichiometric amount of B. In reaction kinetics, d_rn_B is expressed as a volume-specific quantity, which is the partial contribution to the total concentration change of B, $d_rc_B = d_rn_B/V$ and $dc_B = dn_B/V$, respectively. In open systems with constant volume V, $dc_B = d_rc_B + d_ec_B$, where r indicates the *internal* reaction and e indicates the *external* flux of B into the unit volume of the system. At steady state the concentration does not change, $dc_B = 0$, when d_rc_B is compensated for by the external flux of B, $d_rc_B = -d_ec_B$ (Gnaiger 1993b). Alternatively, $dc_B = 0$ when B is held constant by different coupled reactions in which B acts as a substrate or a product.

4*e*: Scalar potential difference across the mitochondrial membrane. In a scalar electric transformation (flux of charge, *i.e.* volume-specific current, from the matrix space to the intermembrane and extramitochondrial space) the motive force is the difference of charge (**Box 2**). The endergonic direction of translocation is defined in **Fig. 2** as $H^+_{in} \rightarrow H^+_{out}$.

5*n*: F = 96.5 (kJ·mol^{-1})/V.

6: The electric partial force is independent of temperature (Note 5), but the chemical partial force depends on absolute temperature, T [K].

6*e*: RT is the gas constant times absolute temperature. ln(10)·RT/F = 59.16 and 61.54 mV at 298.15 and 310.15 K (25 and 37 °C), respectively.

6*n*: ln(10)·RT = 5.708 and 5.938 kJ·mol^{-1} at 298.15 and 310.15 K (25 and 37 °C), respectively.

3.3. Forces and fluxes in physics and irreversible thermodynamics

According to its definition in physics, a potential difference and as such the *protonmotive force*, Δp_{H+}, is not a force *per se* (Cohen *et al.* 2008). The fundamental forces of physics are distinguished from *motive forces* of statistical and irreversible thermodynamics. Complementary to the attempt towards unification of fundamental forces defined in physics,

the concepts of Nobel laureates Lars Onsager, Erwin Schrödinger, Ilya Prigogine and Peter Mitchell (even if expressed in apparently unrelated terms) unite the diversity of *generalized* or 'isomorphic' *flux-force* relationships, the product of which links to the dissipation function and Second Law of thermodynamics (Schrödinger 1944; Prigogine 1967). A *motive force* is the derivative of potentially available or 'free' energy (exergy) per isomorphic *motive* unit (**Box 3**). Perhaps the first account of a *motive force* in energy transformation can be traced back to the Peripatetic school around 300 BC in the context of moving a lever, up to Newton's motive force proportional to the alteration of motion (Coopersmith 2010).

Vectorial and scalar forces, and fluxes: In chemical reactions and osmotic or diffusion processes occurring in a closed heterogeneous system, such as a chamber containing isolated mitochondria, scalar transformations occur without measured spatial direction but between separate compartments (translocation between the matrix and intermembrane space) or between energetically-separated chemical substances (reactions from substrates to products). Hence, the corresponding fluxes are not vectorial but scalar, and are expressed per volume and not per membrane area (**Box 2**). The corresponding motive forces are also scalar potential *differences* across the membrane (**Table 5**), without taking into account the *gradients* across the 6 nm thick inner mitochondrial membrane (Rich 2003).

Coupling: In energetics (ergodynamics), coupling is defined as an energy transformation fuelled by an exergonic (downhill) input process driving the advancement of an endergonic (uphill) output process. The (negative) output/input power ratio is the efficiency of a coupled energy transformation (**Box 4**). At the limit of maximum efficiency of a completely coupled system, the (negative) input power equals the (positive) output power, such that the total power approaches zero at the maximum efficiency of 1, and the process becomes fully reversible without any dissipation of exergy, *i.e.* without entropy production.

872

873 **Box 4: Coupling, power and efficiency, at constant temperature and pressure**

874 Energetic coupling means that two processes of energy transformation are linked such that the
875 input power, P_{in}, is the driving element of the output power, P_{out}, and the out/input power ratio
876 is the efficiency. In general, power is work per unit time [$J.s^{-1}$ = W]. When describing a system
877 with volume V without information on the internal structure, the output is defined as the *external*
878 work (exergy) performed by the *total* system on its environment. Such a system may be open
879 for any type of exchange, or closed and thus allowing only heat and work to be exchanged
880 across the system boundaries. This is the classical black box approach of thermodynamics. In
881 contrast, in a colourful compartmental analysis of *internal* energy transformations (**Fig. 2**), the
882 system is structured and described by definition of ergodynamic compartments (with
883 information on the heterogeneity of the system; **Box 2**) and analysis of separate parts, *i.e.* a
884 sequence of *partial* energy transformations, tr. In general, power per unit volume, P_{tr}/V [$W.L^{-1}$],
885 is the product of a volume-specific flux, J_{tr}, and its conjugated force, F_{tr}, and is closely linked
886 to the dissipation function using the terminology of irreversible thermodynamics (Prigogine
887 1967; Gnaiger 1993a,b). Output power of proton translocation and catabolic input power are
888 (**Fig. 2**),

889 Output: $P_{H+,out}/V = J_{H+,out} \cdot F_{H+,out}$

890 Input: $P_k/V = J_{O2,k} \cdot F_{O2,k}$

891 $F_{O2,k}$ is the exergonic input force with a negative sign, and, $F_{H+,out}$, is the endergonic output
892 force with a positive sign (**Box 3**). Ergodynamic efficiency is the ratio of output/input power,
893 or the flux ratio times force ratio (Gnaiger 1993a,b),

894 $$\varepsilon = \frac{P_{H+,out}}{-P_k} = \frac{J_{H+,out}}{J_{O2,k}} \cdot \frac{F_{H+,out}}{-F_{O2,k}}$$

895 The concept of incomplete coupling relates exclusively to the first term, *i.e.* the flux ratio, or
896 H^+_{out}/O_2 ratio (**Fig. 1**). Likewise, respirometric definitions of the P»/O_2 ratio and biochemical

coupling efficiency (Section 3.2) consider flux ratios. In a completely coupled process, the power efficiency, ε, depends entirely on the force ratio, ranging from zero efficiency at an output force of zero, to the limiting output force and maximum efficiency of 1.0, when the total power of the coupled process, $P_t = P_k + P_{H+,out}$, equals zero, and any net flows are zero at ergodynamic equilibrium of a coupled process. Thermodynamic equilibrium is defined as the state when all potentials (all forces) are dissipated and equilibrate towards their minima of zero. In a fully or completely coupled process, output and input fluxes are directly proportional in a fixed ratio technically defined as a stoichiometric relationship (a gear ratio in a mechanical system). Such maximal stoichiometric output/input flux ratios are considered in OXPHOS analysis as the upper limits or mechanistic H^+_{out}/O_2 and $P\gg/O_2$ ratios (**Fig. 1**).

Coupled versus bound processes: Since the chemiosmotic theory describes the mechanisms of coupling in OXPHOS, it may be interesting to ask if the electrical and chemical parts of proton translocation are coupled processes. This is not the case according to the definition of coupling. If the coupling mechanism is disengaged, the output process becomes independent of the input process, and both proceed in their downhill (exergonic) direction (**Fig. 2**). It is not possible to physically uncouple the electrical and chemical processes, which are only *theoretically* partitioned as electrical and chemical components and can be measured separately. If partial processes are non-separable, *i.e.*, cannot be uncoupled, then these are not *coupled* but are defined as *bound* processes. The electrical and chemical parts are tightly bound partial forces of the protonmotive force, since a flux cannot be partitioned but expressed only in either an electrical or chemical isomorphic format (**Table 4**).

4. Normalization: fluxes and flows

The challenges of measuring mitochondrial respiratory flux are matched by those of normalization, whereby O_2 consumption may be considered as the numerator and normalization

as the complementary denominator, which are tightly linked in reporting the measurements in a format commensurate with the requirements of a database.

4.1. Flux per chamber volume

When the reactor volume does not change during the reaction, which is typical for liquid phase reactions, the volume-specific *flux of a chemical reaction* r is the time derivative of the advancement of the reaction per unit volume, $J_{V,B} = d_r\xi_B/dt \cdot V^{-1}$ [(mol·s^{-1})·L^{-1}]. The *rate of concentration change* is dc_B/dt [(mol·L^{-1})·s^{-1}], where concentration is $c_B = n_B/V$. It is helpful to make the subtle distinction between [mol·s^{-1}·L^{-1}] and [mol·L^{-1}·s^{-1}] for the fundamentally different quantities of volume-specific flux and rate of concentration change, which merge to a single expression only in closed systems. In open systems, external fluxes (such as O_2 supply) are distinguished from internal transformations (metabolic flux, O_2 consumption). In a closed system, external flows of all substances are zero and O_2 consumption (internal flow), I_{O2} [pmol·s^{-1}], causes a decline of the amount of O_2 in the system, n_{O2} [nmol]. Normalization of these quantities for the volume of the system, V [L = dm^3], yields volume-specific O_2 flux, $J_{V,O2} = I_{O2}/V$ [nmol·s^{-1}·L^{-1}], and O_2 concentration, [O_2] or $c_{O2} = n_{O2}/V$ [nmol·mL^{-1} = µmol·L^{-1} = µM]. Instrumental background O_2 flux is due to external flux into a non-ideal closed respirometer, such that total volume-specific flux has to be corrected for instrumental background O_2 flux, *i.e.* O_2 diffusion into or out of the instrumental chamber. $J_{V,O2}$ is relevant mainly for methodological reasons and should be compared with the accuracy of instrumental resolution of background-corrected flux, *e.g.* ±1 nmol·s^{-1}·L^{-1} (Gnaiger 2001). ‘Metabolic’ or catabolic indicates O_2 flux, $J_{O2,k}$, corrected for instrumental background O_2 flux and chemical background O_2 flux due to autoxidation of chemical components added to the incubation medium.

949 *4.2. System-specific and sample-specific normalization*

950 Application of common and generally defined units is required for direct transfer of
951 reported results into a database. The second [s] is the *SI* unit for the base quantity *time*. It is also
952 the standard time-unit used in solution chemical kinetics. **Table 6** lists some conversion factors
953 to obtain *SI* units. The term *rate* is not sufficiently defined to be useful for a database (**Fig. 7**).
954 The inconsistency of the meanings of rate becomes fully apparent when considering Galileo
955 Galilei's famous principle, that 'bodies of different weight all fall at the same rate (have a
956 constant acceleration)' (Coopersmith 2010).

957 **Extensive quantities:** An extensive quantity increases proportionally with system size.
958 The magnitude of an extensive quantity is completely additive for non-interacting subsystems,
959 such as mass or flow expressed per defined system. The magnitude of these quantities depends
960 on the extent or size of the system (Cohen *et al.* 2008).

961

962 **Fig. 7. Different meanings of *rate* may lead to confusion, if the normalization is not sufficiently specified.** Results are frequently expressed as mass-specific *flux*, J_m, per mg protein, dry or wet weight (mass). Cell volume, V_{cell}, or mitochondrial volume, V_{mt}, may be used for normalization (volume-specific flux, J_{Vcell} or J_{Vmt}), which then must be clearly distinguished from flux, J_V, expressed for methodological reasons per volume of the measurement system, or flow per cell, I_X.

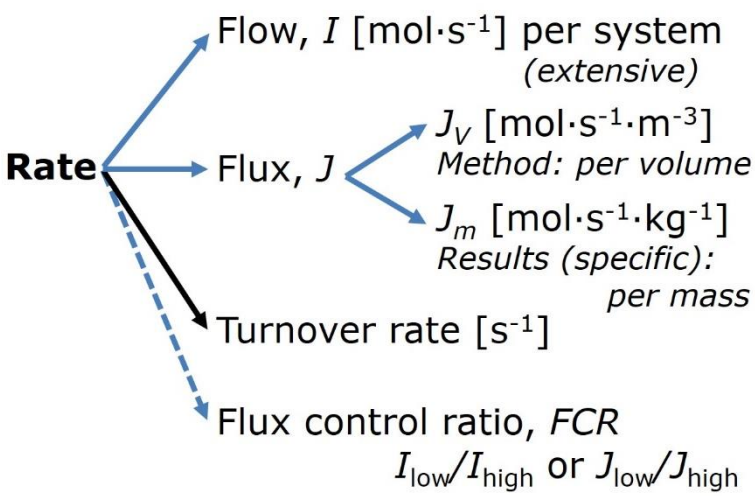

973

974 **Size-specific quantities:** 'The adjective *specific* before the name of an extensive quantity
975 is often used to mean *divided by mass*' (Cohen *et al.* 2008). Mass-specific flux is flow divided
976 by mass of the system. A mass-specific quantity is independent of the extent of non-interacting

977 homogenous subsystems. Tissue-specific quantities are of fundamental interest in comparative
978 mitochondrial physiology, where *specific* refers to the *type* rather than *mass* of the tissue. The
979 term *specific*, therefore, must be further clarified, such that tissue mass-specific, *e.g.*, muscle
980 mass-specific quantities are defined.

981 **Molar quantities:** 'The adjective *molar* before the name of an extensive quantity
982 generally means *divided by amount of substance*' (Cohen *et al.* 2008). The notion that all molar
983 quantities then become *intensive* causes ambiguity in the meaning of *molar Gibbs energy*. It is
984 important to emphasize the fundamental difference between normalization for amount of
985 substance *in a system* or for amount of motive substance *in a transformation*. When the Gibbs
986 energy of a system, G [J], is divided by the amount of substance B in the system, n_B [mol], a
987 *size-specific* molar quantity is obtained, $G_B = G/n_B$ [J·mol^{-1}], which is not any force at all. In
988 contrast, when the partial Gibbs energy change, $\partial_r G$ [J], is divided by the motive amount of
989 substance B in reaction r (advancement of reaction), $\partial_r\xi_B$ [mol], the resulting intensive molar
990 quantity, $F_{B,r} = \partial G/\partial_r\xi_B$ [J·mol^{-1}], is the chemical motive force of reaction r involving 1 mol B
991 (**Table 5**, Note 4).

992 **Flow per system, *I*:** In analogy to electrical terms, flow as an extensive quantity (I; per
993 system) is distinguished from flux as a size-specific quantity (J; per system size) (**Fig. 7**).
994 Electric current is flow, I_{el} [A = C·s^{-1}] per system (extensive quantity). When dividing this
995 extensive quantity by system size (membrane area), a size-specific quantity is obtained, which
996 is electric flux (electric current density), $\boldsymbol{J}_{el}$ [A·m^{-2} = C·s^{-1}·m^{-2}].

997 **Size-specific flux, *J***: Metabolic O_2 flow per tissue increases as tissue mass is increased.
998 Tissue mass-specific O_2 flux should be independent of the size of the tissue sample studied in
999 the instrument chamber, but volume-specific O_2 flux (per volume of the instrument chamber,
1000 V) should increase in direct proportion to the amount of sample in the chamber. Accurate
1001 definition of the experimental system is decisive: whether the experimental chamber is the
1002 closed, open, isothermal or non-isothermal *system* with defined volume as part of the

measurement apparatus, in contrast to the experimental *sample* in the chamber (**Table 6**). Volume-specific O_2 flux depends on mass-concentration of the sample in the chamber, but should be independent of the chamber volume. There are practical limitations to increasing the mass-concentration of the sample in the chamber, when one is concerned about crowding effects and instrumental time resolution.

Sample concentration C_{mX}: Normalization for sample concentration is required for reporting respiratory data. Consider a tissue or cells as the sample, X, and the sample mass, m_X [mg] from which a mitochondrial preparation is obtained. The sample mass is frequently measured as wet or dry weight ($m_X \equiv W_w$ or W_d [mg]), or as amount of tissue or cell protein ($m_X \equiv m_{Protein}$). In the case of permeabilized tissues, cells, and homogenates, the sample concentration, $C_{mX} = m_X/V$ [mg·mL^{-1} = g·L^{-1}], is simply the mass of the subsample of tissue that is transferred into the instrument chamber. Part of the mitochondria from the tissue is lost during preparation of isolated mitochondria, and only a fraction of mitochondria is obtained, expressed as the mitochondrial yield (**Fig. 8**). At a high mitochondrial yield the sample of isolated mitochondria is more representative of the total mitochondrial population than in preparations characterized by low mitochondrial yield. Determination of the mitochondrial yield is based on measurement of the concentration of a mitochondrial marker in the tissue homogenate, $C_{mte,thom}$, which simultaneously provides information on the specific mitochondrial density in the sample (**Fig. 8**).

Tissues can contain multiple cell populations which may have distinct mitochondrial subtypes. Mitochondria are also in a constant state of flux due to highly dynamic fission and fusion cycles, and can exist in multiple stages and sizes which may be altered by a range of factors. The isolation of mitochondria (often achieved through differential centrifugation) can therefore yield a subsample of the mitochondrial types present in a tissue, dependent on isolation protocols utilized (*e.g.* centrifugation speed). This possible artefact should be taken into account when planning experiments using isolated mitochondria. The tendency for

mitochondria of specific sizes to be enriched at different centrifugation speeds also has the potential to allow the isolation of specific mitochondrial subpopulations and therefore the analysis of mitochondria from multiple cell lineages within a single tissue.

Table 6. Sample concentrations and normalization of flux with *SI* base units.

Expression	Symbol	Definition	*SI* Unit	Notes
Sample				
Identity of sample	X	Cells, animals, patients		
Number of sample entities X	N_X	Number of cells, *etc.*	x	
Mass of sample X	m_X		kg	1
Mass of entity X	M_X	$M_X = m_X \cdot N_X^{-1}$	$kg \cdot x^{-1}$	1
Mitochondria				
Mitochondria	mt	X = mt		
Amount of mt-elements	mte	Quantity of mt-marker	x_{mte}	
Concentrations				
Sample number concentration	C_{NX}	$C_{NX} = N_X \cdot V^{-1}$	$x \cdot m^{-3}$	2
Sample mass concentration	C_{mX}	$C_{mX} = m_X \cdot V^{-1}$	$kg \cdot m^{-3}$	
Mitochondrial concentration	C_{mte}	$C_{mte} = mte \cdot V^{-1}$	$x_{mte} \cdot m^{-3}$	3
Specific mitochondrial density	D_{mte}	$D_{mte} = mte \cdot m_X^{-1}$	$x_{mte} \cdot kg^{-1}$	4
Mitochondrial content, mte per entity X	mte_X	$mte_X = mte \cdot N_X^{-1}$	$x_{mte} \cdot x^{-1}$	5
O_2 flow and flux				6
Flow	I_{O2}	Internal flow	$mol \cdot s^{-1}$	7
Volume-specific flux	$J_{V,O2}$	$J_{V,O2} = I_{O2} \cdot V^{-1}$	$mol \cdot s^{-1} \cdot m^{-3}$	8
Flow per sample entity X	$I_{X,O2}$	$I_{X,O2} = J_{V,O2} \cdot C_{NX}^{-1}$	$mol \cdot s^{-1} \cdot x^{-1}$	9
Mass-specific flux	$J_{mX,O2}$	$J_{mX,O2} = J_{V,O2} \cdot C_{mX}^{-1}$	$mol \cdot s^{-1} \cdot kg^{-1}$	
Mitochondria-specific flux	$J_{mte,O2}$	$J_{mte,O2} = J_{V,O2} \cdot C_{mte}^{-1}$	$mol \cdot s^{-1} \cdot x_{mte}^{-1}$	10

1 The *SI* prefix k is used for the SI base unit of mass (kg = 1,000 g). In praxis, various *SI* prefixes are used for convenience, to make numbers easily readable, *e.g.* 1 mg tissue, cell or mitochondrial mass instead of 0.000001 kg.

2 In case X = cells, the sample number concentration is $C_{Ncell} = N_{cell} \cdot V^{-1}$, and volume may be expressed in [dm^3 = L] or [cm^3 = mL]. See **Table 7** for different sample types.

3 mt-concentration is an experimental variable, dependent on sample concentration: (*1*) $C_{mte} = mte \cdot V^{-1}$; (*2*) $C_{mte} = mte_X \cdot C_{NX}$; (*3*) $C_{mte} = C_{mX} \cdot D_{mte}$.

4 If the amount of mitochondria, mte, is expressed as mitochondrial mass, then D_{mte} is the mass fraction of mitochondria in the sample. If mte is expressed as mitochondrial volume, V_{mt}, and the

mass of sample, m_X, is replaced by volume of sample, V_X, then D_{mte} is the volume fraction of mitochondria in the sample.

5 $mte_X = mte \cdot N_X^{-1} = C_{mte} \cdot C_{NX}^{-1}$.

6 Entity O_2 can be replaced by other chemical entities B to study different reactions.

7 I_{O2} and V are defined per instrument chamber as a system of constant volume (and constant temperature), which may be closed or open. I_{O2} is abbreviated for $I_{O2,r}$, *i.e.* the metabolic or internal O_2 flow of the chemical reaction r in which O_2 is consumed, hence the negative stoichiometric number, $\nu_{O2} = -1$. $I_{O2,r} = d_r n_{O2}/dt \cdot \nu_{O2}^{-1}$. If r includes all chemical reactions in which O_2 participates, then $d_r n_{O2} = dn_{O2} - d_e n_{O2}$, where dn_{O2} is the change in the amount of O_2 in the instrument chamber and $d_e n_{O2}$ is the amount of O_2 added externally to the system. At steady state, by definition $dn_{O2} = 0$, hence $d_r n_{O2} = -d_e n_{O2}$.

8 $J_{V,O2}$ is an experimental variable, expressed per volume of the instrument chamber.

9 $I_{X,O2}$ is a physiological variable, depending on the size of entity X.

10 There are many ways to normalize for a mitochondrial marker, that are used in different experimental approaches: (*1*) $J_{mte,O2} = J_{V,O2} \cdot C_{mte}^{-1}$; (*2*) $J_{mte,O2} = J_{V,O2} \cdot C_{mX}^{-1} \cdot D_{mte}^{-1} = J_{mX,O2} \cdot D_{mte}^{-1}$; (*3*) $J_{mte,O2} = J_{V,O2} \cdot C_{NX}^{-1} \cdot mte_X^{-1} = I_{X,O2} \cdot mte_X^{-1}$; (*4*) $J_{mte,O2} = I_{O2} \cdot mte^{-1}$.

Mass-specific flux, $J_{mX,O2}$: Mass-specific flux is obtained by expressing respiration per mass of sample, m_X [mg]. X is the type of sample, *e.g.*, tissue homogenate, permeabilized fibres or cells. Volume-specific flux is divided by mass concentration of X, $J_{mX,O2} = J_{V,O2}/C_{mX}$; or flow per cell is divided by mass per cell, $J_{mcell,O2} = I_{cell,O2}/M_{cell}$. If mass-specific O_2 flux is constant and independent of sample size (expressed as mass), then there is no interaction between the subsystems. A 1.5 mg and a 3.0 mg muscle sample respires at identical mass-specific flux. Mass-specific O_2 flux, however, may change with the mass of a tissue sample, cells or isolated mitochondria in the measuring chamber, in which case the nature of the interaction becomes an issue. Optimization of cell density and arrangement is generally important and particularly in experiments carried out in wells, considering the confluency of the cell monolayer or clumps of cells (Salabei *et al.* 2014).

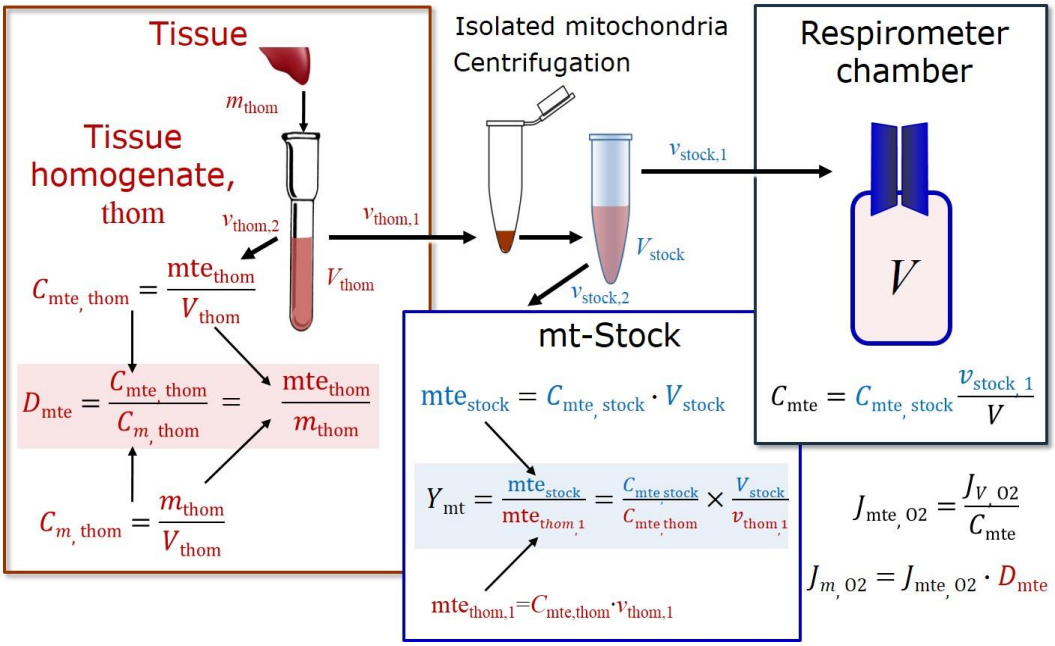

1074

Symbol	Definition [Units]
C_{mte}	Mitochondrial concentration in chamber [$x_{mte} \cdot L^{-1}$]
C_m	Sample mass concentration in chamber [$g \cdot L^{-1}$]
D_{mte}	Specific mte-density per tissue mass [$x_{mte} \cdot g^{-1}$]
$J_{m,O2}$	Mass-specific O_2 flux [$nmol \cdot s^{-1} \cdot g^{-1}$]
$J_{mte,O2}$	Mitochondria-specific O_2 flux [$nmol \cdot s^{-1} \cdot x_{mte}^{-1}$]
mte	Amount of mitochondrial elements [x_{mte}]
m_{thom}	Mass of tissue in the homogenate [g]
Y_{mt}	Yield of isolated mitochondria

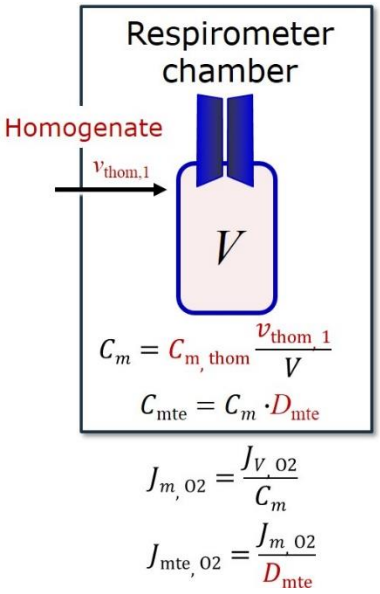

1075

1076 **Fig. 8. Normalization of volume-specific flux of isolated mitochondria and tissue**
1077 **homogenate. A:** Mitochondrial yield, Y_{mt}, in preparation of isolated mitochondria. $v_{thom,1}$
1078 and $v_{stock,1}$ are the volumes transferred from the total volume, V_{thom} and V_{stock}, respectively.
1079 $mte_{thom,1}$ is the amount of mitochondrial elements in volume $v_{thom,1}$ used for isolation. **B:**
1080 In respirometry with homogenate, $v_{thom,1}$ is transferred directly into the respirometer
1081 chamber. See **Table 6** for further explanation of symbols.

1082

1083

1084

Table 7. Some useful abbreviations of various sample types, *X*.

Identity of sample	*X*
Mitochondrial preparation	mtprep
Isolated mitochondria	imt
Tissue homogenate	thom
Permeabilized tissue	pti
Permeabilized fibre	pfi
Permeabilized cell	pce
Cell	ce
Organism	org

Number concentration, C_{NX}: The experimental *number concentration* of sample in the case of cells or animals, *e.g.*, nematodes is $C_{NX} = N_X/V$ [x·mL^{-1}], where N_X is the number of cells or organisms in the chamber (**Table 6**).

Flow per sample entity, $I_{X,O2}$: A special case of normalization is encountered in respiratory studies with permeabilized (or intact) cells. If respiration is expressed per cell, the O_2 flow per measurement system is replaced by the O_2 flow per cell, $I_{cell,O2}$ (**Table 6**). O_2 flow can be calculated from volume-specific O_2 flux, $J_{V,O2}$ [nmol·s^{-1}·L^{-1}] (per V of the measurement chamber [L]), divided by the number concentration of cells, $C_{Nce} = N_{ce}/V$ [cell·L^{-1}], where N_{ce} is the number of cells in the chamber. Cellular O_2 flow can be compared between cells of identical size. To take into account changes and differences in cell size, further normalization is required to obtain cell size-specific or mitochondrial marker-specific O_2 flux (Renner *et al.* 2003).

The complexity changes when the sample is a whole organism studied as an experimental model. The well-established scaling law in respiratory physiology reveals a strong interaction of O_2 consumption and individual body mass of an organism, since *basal* metabolic rate (flow) does not increase linearly with body mass, whereas *maximum* mass-specific O_2 flux, $\dot{V}_{O2max}$ or

$\dot{V}_{O2peak}$, is approximately constant across a large range of individual body mass (Weibel and Hoppeler 2005), with individuals, breeds, and certain species deviating substantially from this general relationship. $\dot{V}_{O2peak}$ of human endurance athletes is 60 to 80 mL $O_2 \cdot min^{-1} \cdot kg^{-1}$ body mass, converted to $J_{m,O2peak}$ of 45 to 60 $nmol \cdot s^{-1} \cdot g^{-1}$ (Gnaiger 2014; **Table 8**).

4.3. Normalization for mitochondrial content

Normalization is a problematic subject and it is essential to consider the question of the study. If the study aims to compare tissue performance, such as the effects of a certain treatment on a specific tissue, then normalization can be successful, using tissue mass or protein content, for example. If the aim, however, is to find differences of mitochondrial function independent of mitochondrial density (**Table 6**), then normalization to a mitochondrial marker is imperative (**Fig. 9**). However, one cannot assume that quantitative changes in various markers such as mitochondrial proteins necessarily occur in parallel with one another. It is important to first establish that the marker chosen is not selectively altered by the performed treatment. In conclusion, the normalization must reflect the question under investigation to reach a satisfying answer. On the other hand, the goal of comparing results across projects and institutions requires some standardization on normalization for entry into a databank.

Mitochondrial concentration, C_{mte}, and mitochondrial markers: It is important that mitochondrial concentration in the tissue and the measurement chamber be quantified, as a physiological output and result of mitochondrial biogenesis and degradation, and as a quantity for normalization in functional analyses. Mitochondrial organelles comprise a cellular reticulum that is in a continual flux of fusion and fission. Hence the definition of an "amount" of mitochondria is often misconceived: mitochondria cannot be counted as a number of occurring elements. Therefore, quantification of the "amount" of mitochondria depends on measurement of chosen mitochondrial markers. ‘Mitochondria are the structural and functional elemental units of cell respiration’ (Gnaiger 2014). The quantity of a mitochondrial marker can

be considered as the measurement of the amount of *elemental mitochondrial units* or *mitochondrial elements*, mte. However, since mitochondrial quality changes under certain stimuli, particularly in mitochondrial dysfunction and after exercise training (Pesta *et al.* 2011; Campos *et al.* 2017), some markers can vary while other markers are unchanged. (*1*) Mitochondrial volume and membrane area are structural markers, whereas mitochondrial protein mass is frequently used as a marker for isolated mitochondria. (*2*) Molecular and enzymatic mitochondrial markers (amounts or activities) can be selected as matrix markers, *e.g.*, citrate synthase activity, mtDNA; or inner mt-membrane markers, *e.g.*, cytochrome *c* oxidase activity, aa_3 content, cardiolipin, TOM20. (*3*) Extending the measurement of mitochondrial marker enzyme activity to mitochondrial pathway capacity, measured as ET or OXPHOS capacity, can be considered as an integrative functional mitochondrial marker.

Depending on the type of mitochondrial marker, the mitochondrial elements, mte, are expressed in marker-specific units. Although concentration and density are used synonymously in physical chemistry, it is recommended to distinguish *experimental mitochondrial concentration*, C_{mte} = mte/V and *physiological mitochondrial density*, D_{mte} = mte/m_X. Then mitochondrial density is the amount of mitochondrial elements per mass of tissue (**Fig. 9**). The former is mitochondrial density multiplied by sample mass concentration, $C_{\mathrm{mte}} = D_{\mathrm{mte}} \cdot C_{mX}$, or mitochondrial content multiplied by sample number concentration, $C_{\mathrm{mte}} = \mathrm{mte}_X \cdot C_{NX}$ (**Table 6**).

Mitochondria-specific flux, $J_{\mathrm{mte,O2}}$: Volume-specific metabolic O_2 flux depends on: (*1*) the sample concentration in the volume of the instrument chamber, C_{mX}, or C_{NX}; (*2*) the mitochondrial density in the sample, D_{mte} = mte/m_X or mte_X = mte/N_X; and (*3*) the specific mitochondrial activity or performance per elemental mitochondrial unit, $J_{\mathrm{mte,O2}} = J_{V,\mathrm{O2}}/C_{\mathrm{mte}}$ (**Table 6**). Obviously, the numerical results for $J_{\mathrm{mte,O2}}$ vary according to the type of mitochondrial marker chosen for measurement of mte and C_{mte} = mte/V.

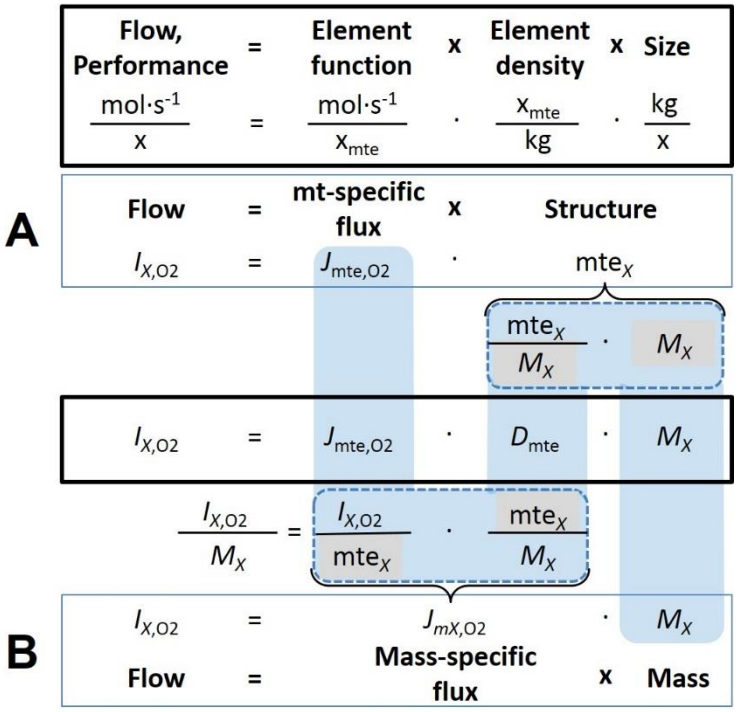

Fig. 9. Structure-function analysis of of performance of a sample entity *X*. O_2 flow, $I_{X,O2}$, as the product of performance per functional element (element function, mitochondria-specific flux), element density (mitochondrial density, D_{mte}), and size of *X* (mass). *X* may be an organism, an organ or tissue, or a cell, with mass M_X. (**A**) Structured analysis: performance is the product of mitochondrial quality (mt-specific flux) and quantity (D_{mte} times size of *X*). (**B**) Unstructured analysis: performance is the product of size-specific flux, $J_{mX,O2} = I_{X,O2}/M_X$, and size (expressed as mass of *X*). See **Table 6** for further explanation of symbols. Modified from Gnaiger (2014).

4.4. Evaluation of mitochondrial markers

Different methods are implicated in quantification of mitochondrial markers and have different strengths. Some problems are common for all mitochondrial markers, mte: (*1*) Accuracy of measurement is crucial, since even a highly accurate and reproducible measurement of O_2 flux results in an inaccurate and noisy expression normalized for a biased

and noisy measurement of a mitochondrial marker. This problem is acute in mitochondrial respiration because the denominators used (the mitochondrial markers) are often very small moieties whose accurate and precise determination is difficult. This problem can be avoided when O_2 fluxes measured in substrate-uncoupler-inhibitor titration protocols are normalized for flux in a defined respiratory reference state, which is used as an *internal* marker and yields flux control ratios, *FCR*s (**Fig. 7**). *FCR*s are independent of any *externally* measured markers and, therefore, are statistically very robust, considering the limitations of ratios in general (Jasienski and Bazzaz 1999). *FCR*s indicate qualitative changes of mitochondrial respiratory control, with highest quantitative resolution, separating the effect of mitochondrial density or concentration on $J_{mX,O2}$ and $I_{X,O2}$ from that of function per elemental mitochondrial marker, $J_{mte,O2}$ (Pesta *et al.* 2011; Gnaiger 2014). (*2*) If mitochondrial quality does not change and only the amount of mitochondria, defined by the chosen mitochondrial marker, varies as a determinant of mass-specific flux, any marker is equally qualified in principle; then in practice selection of the optimum marker depends only on the accuracy and precision of measurement of the mitochondrial marker. (*3*) If mitochondrial flux control ratios change, then there may not be any best mitochondrial marker. In general, measurement of multiple mitochondrial markers enables a comparison and evaluation of normalization for a variety of mitochondrial markers. Evaluation of mitochondrial markers in healthy controls is insufficient for providing guidelines for application in the diagnosis of pathological states and specific treatments.

In line with the concept of the respiratory control ratio (Chance and Williams 1955a), the most readily used normalization is that of flux control ratios and flux control factors (Gnaiger 2014). Selection of the state of maximum flux in a protocol as the reference state has the advantages of (*1*) internal normalization, (*2*) statistical linearization of the response in the range of 0 to 1, and (*3*) consideration of maximum flux for integrating a very large number of elemental steps in the OXPHOS or ET-pathways. This reduces the risk of selecting a functional marker that is specifically altered by the treatment or pathodology, yet increases the chance that

the highly integrative pathway is disproportionately affected, *e.g.* the OXPHOS rather than ET pathway in case of an enzymatic defect in the phosphorylation pathway. In this case, additional information can be obtained by reporting flux control ratios based on a reference state which indicates stable tissue-mass specific flux. Stereological determination of mitochondrial content via two-dimensional transmission electron microscopy can have limitations due to the dynamics of mitochondrial size (Meinild Lundby *et al.* 2017). Accurate determination of three-dimensional volume by two-dimensional microscopy can be both time consuming and statistically challenging (Larsen *et al.* 2012). Using mitochondrial marker enzymes (citrate synthase activity, Complex I–IV amount or activity) for normalization of flux is limited in part by the same factors that apply to the use of flux control ratios. Strong correlations between various mitochondrial markers and citrate synthase activity (Reichmann et al. 1985; Boushel *et al.* 2007; Mogensen *et al.* 2007) are expected in a specific tissue of healthy subjects and in disease states not specifically targeting citrate synthase. Citrate synthase activity is acutely modifiable by exercise (Tonkonogi *et al.* 1997; Leek *et al.* 2001). Evaluation of mitochondrial markers related to a selected age and sex cohort cannot be extrapolated to provide recommendations for normalization in respirometric diagnosis of disease, in different states of development and ageing, different cell types, tissues, and species. mtDNA normalised to nDNA via qPCR is correlated to functional mitochondrial markers including OXPHOS and ET capacity in some cases (Puntschart *et al.* 1995; Wang *et al.* 1999; Menshikova *et al.* 2006; Boushel *et al.* 2007), but lack of such correlations have been reported (Menshikova *et al.* 2005; Schultz and Wiesner 2000; Pesta et al. 2011). Several studies indicate a strong correlation between cardiolipin content and increase in mitochondrial functionality with exercise (Menshikova *et al.* 2005; Menshikova *et al.* 2007; Larsen *et al.* 2012; Faber *et al.* 2014), but its use as a general mitochondrial biomarker in disease remains questionable.

4.5. Conversion: units and normalization

Many different units have been used to report the rate of oxygen consumption, OCR (**Table 8**). *SI* base units provide the common reference for introducing the theoretical principles (**Fig. 7**), and are used with appropriately chosen *SI* prefixes to express numerical data in the most practical format, with an effort towards unification within specific areas of application (**Table 9**). For studies of cells, we recommend that respiration be expressed, as far as possible, as (*1*) O_2 flux normalized for a mitochondrial marker, for separation of the effects of mitochondrial quality and content on cell respiration (this includes *FCR*s as a normalization for a functional mitochondrial marker); (*2*) O_2 flux in units of cell volume or mass, for comparison of respiration of cells with different cell size (Renner *et al.* 2003) and with studies on tissue preparations, and (*3*) O_2 flow in units of attomole (10^{-18} mol) of O_2 consumed by each cell in a second [amol·s^{-1}·$cell^{-1}$], numerically equivalent to [pmol·s^{-1}·10^{-6} cells]. This convention allows information to be easily used when designing experiments in which oxygen consumption must be considered. For example, to estimate the volume-specific O_2 flux in an instrument chamber that would be expected at a particular cell number concentration, one simply needs to multiply the flow per cell by the number of cells per volume of interest. This provides the amount of O_2 [mol] consumed per time [s^{-1}] per unit volume [L^{-1}]. At an O_2 flow of 100 amol·s^{-1}·$cell^{-1}$ and a cell density of 10^9 cells·L^{-1} (10^6 cells·mL^{-1}), the volume-specific O_2 flux is 100 nmol·s^{-1}·L^{-1} (100 pmol·s^{-1}·mL^{-1}).

Although volume is expressed as m^3 using the *SI* base unit, the litre [dm^3] is the basic unit of volume for concentration and is used for most solution chemical kinetics. If one multiplies $I_{cell,O2}$ by C_{Ncell}, then the result will not only be the amount of O_2 [mol] consumed per time [s^{-1}] in one litre [L^{-1}], but also the change in the concentration of oxygen per second (for any volume of an ideally closed system). This is ideal for kinetic modeling as it blends with chemical rate equations where concentrations are typically expressed in mol·L^{-1} (Wagner *et al.* 2011). In studies of multinuclear cells, such as differentiated skeletal muscle cells, it is easy to determine

the number of nuclei but not the total number of cells. A generalized concept, therefore, is obtained by substituting cells by nuclei as the sample entity. This does not hold, however, for enucleated platelets.

Table 8. Conversion of various units used in respirometry and ergometry. e is the number of electrons or reducing equivalents. z_B is the charge number of entity B.

1 Unit	x	Multiplication factor	*SI*-Unit	Note
ng.atom O·s^{-1}	(2 e)	0.5	nmol O_2·s^{-1}	
ng.atom O·min^{-1}	(2 e)	8.33	pmol O_2·s^{-1}	
natom O·min^{-1}	(2 e)	8.33	pmol O_2·s^{-1}	
nmol O_2·min^{-1}	(4 e)	16.67	pmol O_2·s^{-1}	
nmol O_2·h^{-1}	(4 e)	0.2778	pmol O_2·s^{-1}	
mL O_2·min^{-1} at STPD[a]		0.744	µmol O_2·s^{-1}	1
W = J/s at -470 kJ/mol O_2		-2.128	µmol O_2·s^{-1}	
mA = mC·s^{-1}	(z_{H+} = 1)	10.36	nmol H^+·s^{-1}	2
mA = mC·s^{-1}	(z_{O2} = 4)	2.59	nmol O_2·s^{-1}	2
nmol H^+·s^{-1}	(z_{H+} = 1)	0.09649	mA	3
nmol O_2·s^{-1}	(z_{O2} = 4)	0.38594	mA	3

1 At standard temperature and pressure dry (STPD: 0 °C = 273.15 K and 1 atm = 101.325 kPa = 760 mmHg), the molar volume of an ideal gas, V_m, and $V_{m,O2}$ is 22.414 and 22.392 L.mol^{-1} respectively. Rounded to three decimal places, both values yield the conversion factor of 0.744. For comparison at NTPD (20 °C), $V_{m,O2}$ is 24.038 L.mol^{-1}. Note that the *SI* standard pressure is 100 kPa.

2 The multiplication factor is $10^6/(z_B \cdot F)$.

3 The multiplication factor is $z_B \cdot F/10^6$.

4.5. Conversion: oxygen, proton and ATP flux

$J_{O2,k}$ is coupled in mitochondrial steady states to proton cycling, $J_{\infty H+} = J_{H+,out} = J_{H+,in}$ (**Fig. 2**). $J_{H+,out/n}$ and $J_{H+,in/n}$ [nmol·s^{-1}·L^{-1}] are converted into electrical units, $J_{H+,out/e}$ [mC·s^{-1}·L^{-1} = mA·L^{-1}] = $J_{H+,out/n}$ [nmol·s^{-1}·L^{-1}]·F [C·mol^{-1}]·10^{-6} (**Table 4**). At a $J_{H+,out}/J_{O2,k}$ ratio or H^+_{out}/O_2 of 20 (H^+_{out}/O = 10), a volume-specific O_2 flux of 100 nmol·s^{-1}·L^{-1} would correspond to a proton flux of 2,000 nmol H^+_{out}·s^{-1}·L^{-1} or volume-specific current of 193 mA·L^{-1}.

$$J_{V,H+out/e}\ [mA·L^{-1}] = J_{V,H+out/n}·F·10^{-6}\ [nmol·s^{-1}·L^{-1}·mC·nmol^{-1}] \quad \text{(Eq. 3.1)}$$

$$J_{V,H+out/e}\ [mA·L^{-1}] = J_{V,O2}·(H^+_{out}/O_2)·F·10^{-6}\ [mC·s^{-1}·L^{-1} = mA·L^{-1}] \quad \text{(Eq. 3.2)}$$

Table 9. Conversion of units with preservation of numerical values.

Name	Frequently used unit	Equivalent unit	Note
Volume-specific flux, $J_{V,O2}$	pmol·s^{-1}·mL^{-1}	nmol·s^{-1}·L^{-1}	1
	mmol·s^{-1}·L^{-1}	mol·s^{-1}·m^{-3}	
Cell-specific flow, I_{O2}	pmol·s^{-1}·10^{-6} cells	amol·s^{-1}·cell^{-1}	2
	pmol·s^{-1}·10^{-9} cells	zmol·s^{-1}·cell^{-1}	3
Cell number concentration, C_{Nce}	10^6 cells·mL^{-1}	10^9 cells·L^{-1}	
Mitochondrial protein concentration, C_{mte}	0.1 mg·mL^{-1}	0.1 g·L^{-1}	
Mass-specific flux, $J_{m,O2}$	pmol·s^{-1}·mg^{-1}	nmol·s^{-1}·g^{-1}	4
Catabolic power, $P_{O2,k}$	µW·10^{-6} cells	pW·cell^{-1}	1
Volume	1,000 L	m^3 (1,000 kg)	
	L	dm^3 (kg)	
	mL	cm^3 (g)	
	µL	mm^3 (mg)	
	fL	µm^3 (pg)	
Amount of substance concentration	M = mol·L^{-1}	mol·dm^{-3}	

1 pmol: picomole = 10^{-12} mol
2 amol: attomole = 10^{-18} mol
3 zmol: zeptomole = 10^{-21} mol
4 nmol: nanomole = 10^{-9} mol

ET capacity in various human cell types including HEK 293, primary HUVEC and fibroblasts ranges from 50 to 180 amol·s^{-1}·cell^{-1}, measured in intact cells in the noncoupled state (see Gnaiger 2014). At 100 amol·s^{-1}·cell^{-1} corrected for ROX (corresponding to a catabolic power of -48 pW·cell^{-1}), the current across the mt-membranes, I_e, approximates 193 pA·cell^{-1} or 0.2

nA per cell. See Rich (2003) for an extension of quantitative bioenergetics from the molecular to the human scale, with a transmembrane proton flux equivalent to 520 A in an adult at a catabolic power of -110 W. Modelling approaches illustrate the link between proton motive force and currents (Willis *et al.* 2016).For NADH- and succinate-linked respiration, the mechanistic P»/O_2 ratio (referring to the full 4 electron reduction of O_2) is calculated at 20/3.7 and 12/3.7, respectively (Eq. 4) equal to 5.4 and 3.3. The classical P»/O ratios (referring to the 2 electron reduction of 0.5 O_2) are 2.7 and 1.6 (Watt *et al.* 2010), in direct agreement with the measured P»/O ratio for succinate of 1.58 ± 0.02 (Gnaiger *et al.* 2000; for detailed reviews see Wikström and Hummer 2012; Sazanov 2015),

$$P\text{»}/O_2 = (H^+_{out}/O_2)/(H^+_{in}/P\text{»}) \quad \text{(Eq. 4)}$$

In summary (**Fig. 1**),

$$J_{V,P\text{»}}\ [\text{nmol}\cdot\text{s}^{-1}\cdot\text{L}^{-1}] = J_{V,O2}\cdot(H^+_{out}/O_2)/(\ H^+_{in}/P\text{»}) \quad \text{(Eq. 5.1)}$$

$$J_{V,P\text{»}}\ [\text{nmol}\cdot\text{s}^{-1}\cdot\text{L}^{-1}] = J_{V,O2}\cdot(P\text{»}/O_2) \quad \text{(Eq. 5.2)}$$

We consider isolated mitochondria as powerhouses and proton pumps as molecular machines to relate experimental results to energy metabolism of the intact cell. The cellular P»/O_2 based on oxidation of glycogen is increased by the glycolytic (fermentative) substrate-level phosphorylation of 3 P»/Glyc, *i.e.*, 0.5 mol P» for each mol O_2 consumed in the complete oxidation of a mol glycosyl unit (Glyc). Adding 0.5 to the mitochondrial P»/O_2 ratio of 5.4 yields a bioenergetic cell physiological P»/O_2 ratio close to 6. Two NADH equivalents are formed during glycolysis and transported from the cytosol into the mitochondrial matrix, either by the malate-aspartate shuttle or by the glycerophosphate shuttle resulting in different theoretical yield of ATP generated by mitochondria, the energetic cost of which potentially must be taken into account. Considering also substrate-level phosphorylation in the TCA cycle, this high P»/O_2 ratio not only reflects proton translocation and OXPHOS studied in isolation, but integrates mitochondrial physiology with energy transformation in the living cell (Gnaiger 1993a).

5. Conclusions

MitoEAGLE can serve as a gateway to better diagnose mitochondrial respiratory defects linked to genetic variation, age-related health risks, sex-specific mitochondrial performance, lifestyle with its effects on degenerative diseases, and thermal and chemical environment. The present recommendations on coupling control states and rates, linked to the concept of the protonmotive force (Part 1) will be extended in a series of reports on pathway control of mitochondrial respiration, respiratory states in intact cells, and harmonization of experimental procedures.

Box 5: Mitochondrial and cell respiration

Mitochondrial and cell respiration is the process of highly exergonic and exothermic energy transformation in which scalar redox reactions are coupled to vectorial ion translocation across a semipermeable membrane, which separates the small volume of a bacterial cell or mitochondrion from the larger volume of its surroundings. The electrochemical exergy can be partially conserved in the phosphorylation of ADP to ATP or in ion pumping, or dissipated in an electrochemical short-circuit. Respiration is thus clearly distinguished from fermentation as the counterpart of cellular core energy metabolism. Respiration is separated in mitochondrial preparations from the partial contribution of fermentative pathways of the intact cell. According to this definition, residual oxygen consumption, as measured after inhibition of mitochondrial electron transfer, does not belong to the class of catabolic reactions and is, therefore, subtracted from total oxygen consumption to obtain baseline-corrected respiration.

The optimal choice for expressing mitochondrial and cell respiration (**Box 5**) as O_2 flow per biological system, and normalization for specific tissue-markers (volume, mass, protein) and mitochondrial markers (volume, protein, content, mtDNA, activity of marker enzymes,

respiratory reference state) is guided by the scientific question under study. Interpretation of the obtained data depends critically on appropriate normalization, and therefore reporting rates merely as $nmol \cdot s^{-1}$ is discouraged, since it restricts the analysis to intra-experimental comparison of relative (qualitative) differences. Expressing O_2 consumption per cell may not be possible when dealing with tissues. For studies with mitochondrial preparations, we recommend that normalizations be provided as far as possible: (*1*) on a per cell basis as O_2 flow (a biophysical normalization); (*2*) per g cell or tissue protein, or per cell or tissue mass as mass-specific O_2 flux (a cellular normalization); and (*3*) per mitochondrial marker as mt-specific flux (a mitochondrial normalization). With information on cell size and the use of multiple normalizations, maximum potential information is available (Renner *et al.* 2003; Wagner *et al.* 2011; Gnaiger 2014). When using isolated mitochondria, mitochondrial protein is a frequently applied mitochondrial marker, the use of which is basically restricted to isolated mitochondria. Mitochondrial markers, such as citrate synthase activity as an enzymatic matrix marker, provide a link to the tissue of origin on the basis of calculating the mitochondrial yield, *i.e.*, the fraction of mitochondrial marker obtained from a unit mass of tissue.

Acknowledgements

We thank M. Beno for management assistance. Supported by COST Action CA15203 MitoEAGLE and K-Regio project MitoFit (EG).

Competing financial interests: E.G. is founder and CEO of Oroboros Instruments, Innsbruck, Austria.

6. References (*incomplete; www links will be deleted in the final version*)

Altmann R. Die Elementarorganismen und ihre Beziehungen zu den Zellen. Zweite vermehrte Auflage. Verlag Von Veit & Comp, Leipzig 1894;160 pp. - www.mitoeagle.org/index.php/Altmann_1894_Verlag_Von_Veit_%26_Comp

Birkedal R, Laasmaa M, Vendelin M. The location of energetic compartments affects energetic communication in cardiomyocytes. Front Physiol 2014;5:376. doi: 10.3389/fphys.2014.00376. eCollection 2014. PMID: 25324784

Breton S, Beaupré HD, Stewart DT, Hoeh WR, Blier PU. The unusual system of doubly uniparental inheritance of mtDNA: isn't one enough? Trends Genet 2007;23:465-74.

Brown GC. Control of respiration and ATP synthesis in mammalian mitochondria and cells. Biochem J 1992;284:1-13. - www.mitoeagle.org/index.php/Brown_1992_Biochem_J

Campos JC, Queliconi BB, Bozi LHM, Bechara LRG, Dourado PMM, Andres AM, Jannig PR, Gomes KMS, Zambelli VO, Rocha-Resende C, Guatimosim S, Brum PC, Mochly-Rosen D, Gottlieb RA, Kowaltowski AJ, Ferreira JCB. Exercise reestablishes autophagic flux and mitochondrial quality control in heart failure. Autophagy 2017;13:1304-317.

Chance B, Williams GR. Respiratory enzymes in oxidative phosphorylation. I. Kinetics of oxygen utilization. J Biol Chem 1955a;217:383-93. - http://www.mitoeagle.org/index.php/Chance_1955_J_Biol_Chem-I

Chance B, Williams GR. Respiratory enzymes in oxidative phosphorylation: III. The steady state. J Biol Chem 1955b;217:409-27. - www.mitoeagle.org/index.php/Chance_1955_J_Biol_Chem-III

Chance B, Williams GR. Respiratory enzymes in oxidative phosphorylation. IV. The respiratory chain. J Biol Chem 1955c;217:429-38. - www.mitoeagle.org/index.php/Chance_1955_J_Biol_Chem-IV

Chance B, Williams GR. The respiratory chain and oxidative phosphorylation. Adv Enzymol Relat Subj Biochem 1956;17:65-134. - www.mitoeagle.org/index.php/Chance_1956_Adv_Enzymol_Relat_Subj_Biochem

Cobb LJ, Lee C, Xiao J, Yen K, Wong RG, Nakamura HK, Mehta HH, Gao Q, Ashur C, Huffman DM, Wan J, Muzumdar R, Barzilai N, Cohen P. Naturally occurring

mitochondrial-derived peptides are age-dependent regulators of apoptosis, insulin sensitivity, and inflammatory markers. Aging (Albany NY) 2016;8:796-809.

Cohen ER, Cvitas T, Frey JG, Holmström B, Kuchitsu K, Marquardt R, Mills I, Pavese F, Quack M, Stohner J, Strauss HL, Takami M, Thor HL. Quantities, units and smbols in physical chemistry, IUPAC Green Book 2008;3rd Edition, 2nd Printing, IUPAC & RSC Publishing, Cambridge. - www.mitoeagle.org/index.php/Cohen_2008_IUPAC_Green_Book

Cooper H, Hedges LV, Valentine JC (eds). The handbook of research synthesis and meta-analysis. Russell Sage Foundation 2009.

Coopersmith J. Energy, the subtle concept. The discovery of Feynman's blocks from Leibnitz to Einstein. Oxford University Press 2010;400 pp.

Cummins J. Mitochondrial DNA in mammalian reproduction. Rev Reprod 1998;3:172–82.

Dai Q, Shah AA, Garde RV, Yonish BA, Zhang L, Medvitz NA, Miller SE, Hansen EL, Dunn CN, Price TM. A truncated progesterone receptor (PR-M) localizes to the mitochondrion and controls cellular respiration. Mol Endocrinol 2013;27:741-53.

Duarte FV, Palmeira CM, Rolo AP. The role of microRNAs in mitochondria: small players acting wide. Genes (Basel) 2014;5:865-86.

Dufour S, Rousse N, Canioni P, Diolez P. Top-down control analysis of temperature effect on oxidative phosphorylation. Biochem J 1996;314:743-51.

Ernster L, Schatz G Mitochondria: a historical review. J Cell Biol 1981;91:227s-55s. - www.mitoeagle.org/index.php/Ernster_1981_J_Cell_Biol

Estabrook RW. Mitochondrial respiratory control and the polarographic measurement of ADP:O ratios. Methods Enzymol 1967;10:41-7. - www.mitoeagle.org/index.php/Estabrook_1967_Methods_Enzymol

Faber C, Zhu ZJ, Castellino S, Wagner DS, Brown RH, Peterson RA, Gates L, Barton J, Bickett M, Hagerty L, Kimbrough C, Sola M, Bailey D, Jordan H, Elangbam CS.

Cardiolipin profiles as a potential biomarker of mitochondrial health in diet-induced obese mice subjected to exercise, diet-restriction and ephedrine treatment. J Appl Toxicol 2014;34:1122-9.

Fell D. Understanding the control of metabolism. Portland Press 1997.

Garlid KD, Semrad C, Zinchenko V. Does redox slip contribute significantly to mitochondrial respiration? In: Schuster S, Rigoulet M, Ouhabi R, Mazat J-P (eds) Modern trends in biothermokinetics. Plenum Press, New York, London 1993;287-93.

Gerö D, Szabo C. Glucocorticoids suppress mitochondrial oxidant production via upregulation of uncoupling protein 2 in hyperglycemic endothelial cells. PLoS One 2016;11:e0154813.

Gnaiger E. Efficiency and power strategies under hypoxia. Is low efficiency at high glycolytic ATP production a paradox? In: Surviving Hypoxia: Mechanisms of Control and Adaptation. Hochachka PW, Lutz PL, Sick T, Rosenthal M, Van den Thillart G (eds.) CRC Press, Boca Raton, Ann Arbor, London, Tokyo 1993a:77-109. - www.mitoeagle.org/index.php/Gnaiger_1993_Hypoxia

Gnaiger E. Nonequilibrium thermodynamics of energy transformations. Pure Appl Chem 1993b;65:1983-2002. - www.mitoeagle.org/index.php/Gnaiger_1993_Pure_Appl_Chem

Gnaiger E. Bioenergetics at low oxygen: dependence of respiration and phosphorylation on oxygen and adenosine diphosphate supply. Respir Physiol 2001;128:277-97. - www.mitoeagle.org/index.php/Gnaiger_2001_Respir_Physiol

Gnaiger E. Mitochondrial pathways and respiratory control. An introduction to OXPHOS analysis. 4th ed. Mitochondr Physiol Network 2014;19.12. Oroboros MiPNet Publications, Innsbruck:80 pp. - www.mitoeagle.org/index.php/Gnaiger_2014_MitoPathways

Gnaiger E. Capacity of oxidative phosphorylation in human skeletal muscle. New perspectives of mitochondrial physiology. Int J Biochem Cell Biol 2009;41:1837-45. - www.mitoeagle.org/index.php/Gnaiger_2009_Int_J_Biochem_Cell_Biol

Gnaiger E, Méndez G, Hand SC. High phosphorylation efficiency and depression of uncoupled respiration in mitochondria under hypoxia. Proc Natl Acad Sci USA 2000;97:11080-5. - www.mitoeagle.org/index.php/Gnaiger_2000_Proc_Natl_Acad_Sci_U_S_A

Greggio C, Jha P, Kulkarni SS, Lagarrigue S, Broskey NT, Boutant M, Wang X, Conde Alonso S, Ofori E, Auwerx J, Cantó C, Amati F. Enhanced respiratory chain supercomplex formation in response to exercise in human skeletal muscle. Cell Metab 2017;25:301-11. - http://www.mitoeagle.org/index.php/Greggio_2017_Cell_Metab

Hofstadter DR. Gödel, Escher, Bach: An eternal golden braid. A metaphorical fugue on minds and machines in the spirit of Lewis Carroll. Harvester Press 1979;499 pp. - www.mitoeagle.org/index.php/Hofstadter_1979_Harvester_Press

Illaste A, Laasmaa M, Peterson P, Vendelin M. Analysis of molecular movement reveals latticelike obstructions to diffusion in heart muscle cells. Biophys J 2012;102:739-48. - PMID: 22385844

Jasienski M, Bazzaz FA. The fallacy of ratios and the testability of models in biology. Oikos 1999;84:321-26.

Jepihhina N, Beraud N, Sepp M, Birkedal R, Vendelin M. Permeabilized rat cardiomyocyte response demonstrates intracellular origin of diffusion obstacles. Biophys J 2011;101:2112-21. - PMID: 22067148

Klepinin A, Ounpuu L, Guzun R, Chekulayev V, Timohhina N, Tepp K, Shevchuk I, Schlattner U, Kaambre T. Simple oxygraphic analysis for the presence of adenylate kinase 1 and 2 in normal and tumor cells. J Bioenerg Biomembr 2016;48:531-48. - http://www.mitoeagle.org/index.php/Klepinin_2016_J_Bioenerg_Biomembr

Klingenberg M. UCP1 - A sophisticated energy valve. Biochimie 2017;134:19-27

Koit A, Shevchuk I, Ounpuu L, Klepinin A, Chekulayev V, Timohhina N, Tepp K, Puurand M,Truu L, Heck K, Valvere V, Guzun R, Kaambre T. Mitochondrial respiration in human colorectal and breast cancer clinical material is regulated differently. Oxid Med Cell Longev 2017;1372640. - http://www.mitoeagle.org/index.php/Koit_2017_Oxid_Med_Cell_Longev

Komlódi T, Tretter L. Methylene blue stimulates substrate-level phosphorylation catalysed by succinyl-CoA ligase in the citric acid cycle. Neuropharmacology 2017;123:287-98. - www.mitoeagle.org/index.php/Komlodi_2017_Neuropharmacology

Lane N. Power, sex, suicide: Mitochondria and the meaning of life. Oxford University Press 2005;354 pp.

Larsen S, Nielsen J, Neigaard Nielsen C, Nielsen LB, Wibrand F, Stride N, Schroder HD, Boushel RC, Helge JW, Dela F, Hey-Mogensen M. Biomarkers of mitochondrial content in skeletal muscle of healthy young human subjects. J Physiol 590;2012:3349-60. - http://www.mitoeagle.org/index.php/Larsen_2012_J_Physiol

Lee C, Zeng J, Drew BG, Sallam T, Martin-Montalvo A, Wan J, Kim SJ, Mehta H, Hevener AL, de Cabo R, Cohen P. The mitochondrial-derived peptide MOTS-c promotes metabolic homeostasis and reduces obesity and insulin resistance. Cell Metab 2015;21:443-54.

Lee SR, Kim HK, Song IS, Youm J, Dizon LA, Jeong SH, Ko TH, Heo HJ, Ko KS, Rhee BD, Kim N, Han J. Glucocorticoids and their receptors: insights into specific roles in mitochondria. Prog Biophys Mol Biol 2013;112:44-54.

Leek BT, Mudaliar SR, Henry R, Mathieu-Costello O, Richardson RS. Effect of acute exercise on citrate synthase activity in untrained and trained human skeletal muscle. Am J Physiol Regul Integr Comp Physiol 2001;280:R441-7.

1492 Lemieux H, Blier PU, Gnaiger E. Remodeling pathway control of mitochondrial respiratory
1493 capacity by temperature in mouse heart: electron flow through the Q-junction in
1494 permeabilized fibers. Sci Rep 2017;7:2840. -
1495 www.mitoeagle.org/index.php/Lemieux_2017_Sci_Rep
1496 Lenaz G, Tioli G, Falasca AI, Genova ML. Respiratory supercomplexes in mitochondria. In:
1497 Mechanisms of primary energy trasduction in biology. M Wikstrom (ed) Royal Society
1498 of Chemistry Publishing, London, UK 2017:296-337 (in press)
1499 Margulis L. Origin of eukaryotic cells. New Haven: Yale University Press 1970.
1500 Meinild Lundby AK, Jacobs RA, Gehrig S, de Leur J, Hauser M, Bonne TC, Flück D,
1501 Dandanell S, Kirk N, Kaech A, Ziegler U, Larsen S, Lundby C. Exercise training
1502 increases skeletal muscle mitochondrial volume density by enlargement of existing
1503 mitochondria and not de novo biogenesis. Acta Physiol (Oxf) 2017;[Epub ahead of
1504 print].
1505 Menshikova EV, Ritov VB, Fairfull L, Ferrell RE, Kelley DE, Goodpaster BH. Effects of
1506 exercise on mitochondrial content and function in aging human skeletal muscle. J
1507 Gerontol A Biol Sci Med Sci 2006;61:534-40.
1508 Menshikova EV, Ritov VB, Ferrell RE, Azuma K, Goodpaster BH, Kelley DE.
1509 Characteristics of skeletal muscle mitochondrial biogenesis induced by moderate-
1510 intensity exercise and weight loss in obesity. J Appl Physiol (1985) 2007;103:21-7.
1511 Menshikova EV, Ritov VB, Toledo FG, Ferrell RE, Goodpaster BH, Kelley DE. Effects of
1512 weight loss and physical activity on skeletal muscle mitochondrial function in obesity.
1513 Am J Physiol Endocrinol Metab 2005;288:E818-25.
1514 Miller GA. The science of words. Scientific American Library New York 1991;276 pp. -
1515 www.mitoeagle.org/index.php/Miller_1991_Scientific_American_Library

Mitchell P. Chemiosmotic coupling in oxidative and photosynthetic phosphorylation Biochim Biophys Acta Bioenergetics 2011;1807:1507-38. - http://www.sciencedirect.com/science/article/pii/S0005272811002283

Mitchell P, Moyle J. Respiration-driven proton translocation in rat liver mitochondria. Biochem J 1967;105:1147-62. - www.mitoeagle.org/index.php/Mitchell_1967_Biochem_J

Mogensen M, Sahlin K, Fernström M, Glintborg D, Vind BF, Beck-Nielsen H, Højlund K. Mitochondrial respiration is decreased in skeletal muscle of patients with type 2 diabetes. Diabetes 2007;56:1592-9.

Moreno M, Giacco A, Di Munno C, Goglia F. Direct and rapid effects of 3,5-diiodo-L-thyronine (T2). Mol Cell Endocrinol 2017;7207:30092-8.

Morrow RM, Picard M, Derbeneva O, Leipzig J, McManus MJ, Gouspillou G, Barbat-Artigas S, Dos Santos C, Hepple RT, Murdock DG, Wallace DC. Mitochondrial energy deficiency leads to hyperproliferation of skeletal muscle mitochondria and enhanced insulin sensitivity. Proc Natl Acad Sci U S A 2017;114:2705-10. - www.mitoeagle.org/index.php/Morrow_2017_Proc_Natl_Acad_Sci_U_S_A

Nicholls DG, Ferguson S. Bioenergetics 4. Elsevier 2013.

Paradies G, Paradies V, De Benedictis V, Ruggiero FM, Petrosillo G. Functional role of cardiolipin in mitochondrial bioenergetics. Biochim Biophys Acta 2014;1837:408-17. - http://www.mitoeagle.org/index.php/Paradies_2014_Biochim_Biophys_Acta

Pesta D, Hoppel F, Macek C, Messner H, Faulhaber M, Kobel C, Parson W, Burtscher M, Schocke M, Gnaiger E. Similar qualitative and quantitative changes of mitochondrial respiration following strength and endurance training in normoxia and hypoxia in sedentary humans. Am J Physiol Regul Integr Comp Physiol 2011;301:R1078–87.

Price TM, Dai Q. The Role of a Mitochondrial Progesterone Receptor (PR-M) in Progesterone Action. Semin Reprod Med. 2015;33:185-94.

Prigogine I. Introduction to thermodynamics of irreversible processes. Interscience, New York, 1967;3rd ed.

Puchowicz MA, Varnes ME, Cohen BH, Friedman NR, Kerr DS, Hoppel CL. Oxidative phosphorylation analysis: assessing the integrated functional activity of human skeletal muscle mitochondria – case studies. Mitochondrion 2004;4:377-85. - www.mitoeagle.org/index.php/Puchowicz_2004_Mitochondrion

Puntschart A, Claassen H, Jostarndt K, Hoppeler H, Billeter R. mRNAs of enzymes involved in energy metabolism and mtDNA are increased in endurance-trained athletes. Am J Physiol 1995;269:C619-25.

Quiros PM, Mottis A, Auwerx J. Mitonuclear communication in homeostasis and stress. Nat Rev Mol Cell Biol 2016;17:213-26.

Reichmann H, Hoppeler H, Mathieu-Costello O, von Bergen F, Pette D. Biochemical and ultrastructural changes of skeletal muscle mitochondria after chronic electrical stimulation in rabbits. Pflugers Arch 1985;404:1-9.

Renner K, Amberger A, Konwalinka G, Gnaiger E. Changes of mitochondrial respiration, mitochondrial content and cell size after induction of apoptosis in leukemia cells. Biochim Biophys Acta 2003;1642:115-23. - www.mitoeagle.org/index.php/Renner_2003_Biochim_Biophys_Acta

Rich P. Chemiosmotic coupling: The cost of living. Nature 2003;421:583. - www.mitoeagle.org/index.php/Rich_2003_Nature

Rostovtseva TK, Sheldon KL, Hassanzadeh E, Monge C, Saks V, Bezrukov SM, Sackett DL. Tubulin binding blocks mitochondrial voltage-dependent anion channel and regulates respiration. Proc Natl Acad Sci USA 2008;105:18746-51. - www.mitoeagle.org/index.php/Rostovtseva_2008_Proc_Natl_Acad_Sci_U_S_A

Rustin P, Parfait B, Chretien D, Bourgeron T, Djouadi F, Bastin J, Rötig A, Munnich A. Fluxes of nicotinamide adenine dinucleotides through mitochondrial membranes in human cultured cells. J Biol Chem 1996;271:14785-90.

Saks VA, Veksler VI, Kuznetsov AV, Kay L, Sikk P, Tiivel T, Tranqui L, Olivares J, Winkler K, Wiedemann F, Kunz WS. Permeabilised cell and skinned fiber techniques in studies of mitochondrial function in vivo. Mol Cell Biochem 1998;184:81-100. - http://www.mitoeagle.org/index.php/Saks_1998_Mol_Cell_Biochem

Salabei JK, Gibb AA, Hill BG. Comprehensive measurement of respiratory activity in permeabilized cells using extracellular flux analysis. Nat Protoc 2014;9:421-38.

Sazanov LA. A giant molecular proton pump: structure and mechanism of respiratory complex I. Nat Rev Mol Cell Biol 2015;16:375-88. - www.mitoeagle.org/index.php/Sazanov_2015_Nat_Rev_Mol_Cell_Biol

Schneider TD. Claude Shannon: biologist. The founder of information theory used biology to formulate the channel capacity. IEEE Eng Med Biol Mag 2006;25:30-3.

Schönfeld P, Dymkowska D, Wojtczak L. Acyl-CoA-induced generation of reactive oxygen species in mitochondrial preparations is due to the presence of peroxisomes. Free Radic Biol Med 2009;47:503-9.

Schrödinger E. What is life? The physical aspect of the living cell. Cambridge Univ Press, 1944. - www.mitoeagle.org/index.php/Gnaiger_1994_BTK

Schultz J, Wiesner RJ. Proliferation of mitochondria in chronically stimulated rabbit skeletal muscle--transcription of mitochondrial genes and copy number of mitochondrial DNA. J Bioenerg Biomembr 2000;32:627-34.

Simson P, Jepihhina N, Laasmaa M, Peterson P, Birkedal R, Vendelin M. Restricted ADP movement in cardiomyocytes: Cytosolic diffusion obstacles are complemented with a small number of open mitochondrial voltage-dependent anion channels. J Mol Cell Cardiol 2016;97:197-203. - PMID: 27261153

1592 Stucki JW, Ineichen EA. Energy dissipation by calcium recycling and the efficiency of
1593 calcium transport in rat-liver mitochondria. Eur J Biochem 1974;48:365-75.
1594 Tonkonogi M, Harris B, Sahlin K. Increased activity of citrate synthase in human skeletal
1595 muscle after a single bout of prolonged exercise. Acta Physiol Scand 1997;161:435-6.
1596 Waczulikova I, Habodaszova D, Cagalinec M, Ferko M, Ulicna O, Mateasik A, Sikurova L,
1597 Ziegelhöffer A. Mitochondrial membrane fluidity, potential, and calcium transients in
1598 the myocardium from acute diabetic rats. Can J Physiol Pharmacol 2007;85:372-81.
1599 Wagner BA, Venkataraman S, Buettner GR. The rate of oxygen utilization by cells. Free
1600 Radic Biol Med. 2011:51:700-712.
1601 http://dx.doi.org/10.1016/j.freeradbiomed.2011.05.024 PMCID: PMC3147247
1602 Wang H, Hiatt WR, Barstow TJ, Brass EP. Relationships between muscle mitochondrial
1603 DNA content, mitochondrial enzyme activity and oxidative capacity in man: alterations
1604 with disease. Eur J Appl Physiol Occup Physiol 1999;80:22-7.
1605 Watt IN, Montgomery MG, Runswick MJ, Leslie AG, Walker JE. Bioenergetic cost of
1606 making an adenosine triphosphate molecule in animal mitochondria. Proc Natl Acad Sci
1607 U S A 2010;107:16823-7. -
1608 www.mitoeagle.org/index.php/Watt_2010_Proc_Natl_Acad_Sci_U_S_A
1609 Weibel ER, Hoppeler H. Exercise-induced maximal metabolic rate scales with muscle aerobic
1610 capacity. J Exp Biol 2005;208:1635–44.
1611 White DJ, Wolff JN, Pierson M, Gemmell NJ. Revealing the hidden complexities of mtDNA
1612 inheritance. Mol Ecol 17; 2008:4925–42.
1613 Wikström M, Hummer G. Stoichiometry of proton translocation by respiratory complex I and
1614 its mechanistic implications. Proc Natl Acad Sci U S A 2012;109:4431-6. -
1615 www.mitoeagle.org/index.php/Wikstroem_2012_Proc_Natl_Acad_Sci_U_S_A
1616 Willis WT, Jackman MR, Messer JI, Kuzmiak-Glancy S, Glancy B. A simple hydraulic
1617 analog model of oxidative phosphorylation. Med Sci Sports Exerc. 2016;48:990-1000.